IEEE Access
Multidisciplinary | Rapid Review | Open Access Journal

Received January 21, 2020, accepted February 19, 2020, date of publication March 3, 2020, date of current version March 26, 2020.

Digital Object Identifier 10.1109/ACCESS.2020.2978121

Solar PV and Biomass Resources-Based Sustainable Energy Supply for Off-Grid Cellular Base Stations

MD. SANWAR HOSSAIN[1], (Student Member, IEEE), ABU JAHID[2], (Student Member, IEEE), KHONDOKER ZIAUL ISLAM[3], AND MD. FAYZUR RAHMAN[4]

[1]Department of Electrical, Electronic, and Communication Engineering, Military Institute of Science and Technology, Dhaka 1216, Bangladesh
[2]Department of Electrical and Computer Engineering, University of Ottawa, Ottawa, ON K1N 6N5, Canada
[3]Department of Electrical and Electronic Engineering, Bangladesh University of Business and Technology, Dhaka 1216, Bangladesh
[4]Department of Electrical and Electronic Engineering, Green University of Bangladesh, Dhaka 1205, Bangladesh

Corresponding author: Md. Sanwar Hossain (sanwareee@gmail.com)

ABSTRACT Due to the technological revolution and higher user data demand, the telecommunication industry is expanding at an exponential rate. Fulfilling the increasing demand of energy for the rising cellular networks has become a great challenge to the network operators because of the limited reservation of fuel energy sources and the growing concern about global warming. Energy harvesting (EH) from renewable energy sources (RES) has become an overwhelming initiative to minimize energy deficiency and carbon footprints. This paper investigates the feasibility of solar photovoltaic (PV) and biomass resources based hybrid supply systems for powering the off-grid Long Term Evolution (LTE) cellular macrocell base stations (BSs) in Bangladesh focusing the technical, economic and environmental issues. In addition, the green energy sharing technique has been incorporated via a low resistive path for optimal use of RES. The proposed system has enough potential to achieve long term sustainability and reduction of pollution rates by fulfilling the future energy demand of BS. In this work, Hybrid Optimization Model for Electric Renewables (HOMER) simulation-based feasibility analysis is used to assess the optimal system, energy production, total net present cost (NPC), cost of electricity (COE) and greenhouse gas (GHG) emission depending on different system parameters. Furthermore, the performance of the network has been evaluated in terms of throughput and energy efficiency using Matlab-based Monte Carlo simulations. Results demonstrate that the proposed hybrid renewable energy powered BSs would be a reliable and longer-lasting green solution for the telecom sector while maintaining the quality of service (QoS). Finally, an extensive comparison with other systems has also been done to justify network validity.

INDEX TERMS Biomass energy, energy efficiency, energy sharing, hybrid power supply, LTE, renewable-energy-powered BSs, solar energy, sustainability.

I. INTRODUCTION

With the remarkable increase in the number of mobile subscribers and high-speed data demand, cellular network operators are deploying a higher number of base stations throughout the world. According to the Ericsson survey, the number of the global mobile subscriber up to the first quarter of 2019 was around 7.9 billion, with 44 million new subscribers added during this quarter, wherein LTE subscribers are 3.7 billion [1]. Currently, Bangladesh has 88 million unique subscribers and it is expected that at the end of 2025, this value will be 107 million [2]. Global System for Mobile Communications Association (GSMA) mentiones that at present, the number of universal BSs is above 4 million and it is nearly double from 2007 to 2012 [3]. Base stations are the premier energy consumer of mobile networks which receive 57% of the total consumed energy [4], [5]. Over the last decades, the exponential evolution of information and communication technology (ICT) has significantly increased the power consumption by cellular networks [6]. In the year of 2007, the annual worldwide consumption of electricity by the telecom industry was 219 TWh that increased to 354 TWh in the year 2012 [7]. It is hoped that energy consumption will be escalated at an additional yearly rate of 10%

The associate editor coordinating the review of this manuscript and approving it for publication was Giovanni Pau.

from 2013 to 2019. Till 2017 [8], Bangladesh has above 36679 GSM BSs, which consume around 642 million kWh of energy and within this 14% BSs are off-grid. Additionally, 81% of the off-grid BSs in Bangladesh are powered by a diesel generator (DG) plus battery system [8]. The International Energy Agency (IEA) has just released its latest global energy projection named the World Energy Outlook 2018 (WEO2018) where global energy demand is expected to grow by around 27% equivalent to 3,743 million tons oil from 2017 to 2040 [9]. According to [10], the information and communication technology (ICT) sector consumes about 5%-10% of universal electricity production and produces about 2% to 4% of global CO_2 outflow, wherein BSs consume about 60% to 80% of the electricity consumed by the ICT sector.

Fulfilling the rapidly increasing demand of energy demand from the non-renewable energy sources has a hostile influence on both the economic and environmental implications resulting in higher capital cost and growth of greenhouse gas emission [11], [12]. As a result, green energy harvesting from different energy sources locally available has become an area of deep attention of the researchers with the aim to produce sustainable and environment-friendly energy [13]–[16]. Locally available green energy sources such as sunlight, biomass, hydro, wind, etc. are re-useable, cheap, and pure in comparison with the non-renewable energy sources. Besides, renewable energy sources are available in many areas throughout the year. Renewable energy source becomes reliable if we can fulfill any of the following conditions. Firstly, it is to be combined with the conventional non-renewable energy source. Secondly, the hybridization of two/three RE sources can also ensure reliability. Thirdly, it achieves reliability if a single RE source is connected with a sufficient battery unit. Finally, renewable energy source becomes reliable when it is tied with the grid.

Meanwhile, power generation from renewable energy sources has become cost-effective, sustainable, and reliable due to technological advancement [17]. Being inspired by the above potential benefits, Australia aims to achieve a renewable energy target of 20% at the end of 2020 to minimize the greenhouse gas emissions by maximum utilization of green energy [18]. In [13], [19], authors examine the feasibility of deploying renewable energy-based cellular networks in different regions around the world and report that approximately 320100 renewable energy-based off-grid BSs have been installed till 2014 and around 389800 green energy-enabled off-grid BSs will be in function within 2020.

Bangladesh is a tropical country which is situated between 20°34′ and 26°38′ north latitude and 88°01′ and 92°41′ east longitude with an area of 147570 km^2 [20]. Bangladesh has the enormous potential of green energy generation from solar and biomass energy sources that create great opportunities for the fulfillment of present and future power demand. According to the National Aeronautics and Space Administration (NASA) Surface Meteorology and Solar Energy Database, the daily solar intensity of the country remain in the range of 4-6.5 kWh/m^2 with average solar radiation of 4.59 $kWh/m^2/day$ [21]. It has been reported that Bangladesh obtains around 70 PWh of solar energy each year which is 3000 times higher than the total electrical energy generation of the country [22]. Being motivated by the above potential solution, solar PV supplied base station has already been established in Bangladesh [23], [24]. Authors in [13] mentioned that up to 2015 above 521 solar PV powered base stations have already been installed in Bangladesh and telecom operators are trying to enhance the figure.

In the meantime, biomass is the fourth greatest energy source in the world, which contributes around 8.5% of the total world energy. In 2012, the United State produced around 15 GW power from biomass which is almost 18% of the total biomass generated power in the world [25]. It is expected that within the next century, almost 50% of the world energy requirement will be supplied by biomass energy [26]. Nowadays, Bangladesh has also started generating energy from biomass on a small scale though most of the energy generated from the biomass is used for cooking and heating purposes only. Energy generation from biomass resources has a huge scope for Bangladesh because of the low cost of biomass residue and the high efficiency of energy conversion. At the same time, agriculture residue is the key source of biomass energy in Bangladesh where rice-husk constitutes a significant amount [27]. Bangladesh produced 51.8 million tons of rice in the financial year (FY) 2014-15 as mentioned by the Food and Agriculture Organization (FAO) [28]. The country annually produces 10 million tons of rice shell from 50 million tons of paddy. As reported by the 'Rice Mills Owners Association' in Bangladesh, there are around 540 rice mills throughout the country with an average capacity of 30 tons/day. They also report that 540 rice mills have the potential of producing 171 MW per day [29], [30]. According to [25], Bangladesh had approximate 90.21 million tons' biomass available in FY 2012-2013 whose energy potential is 1344.99 PJ equivalent to 373.71 TWh. Authors in [28] studied that Bangladesh will be able to generate 7682 GWh energy from the rice husk with a total capacity of 1066 MW in 2030. Moreover, around 13% of the total primary energy consumption came from renewable energy sources in 2012 [25]. Finally, GSMA reported that Bangladesh can save around 90 million USD per year by installing green energy harvesting technology instead of using the fossil fuel-based energy generation system [8].

It is always desirable to develop an energy-efficient green cellular network, which will minimize the capital cost, and greenhouse gas emission by maintaining the quality of services. Improving energy efficiency (EE) and maintaining QoS is quite challenging in the process of deploying renewable energy (RE) focused BSs [31], [32]. For example, energy harvesting from the green energy sources is greatly affected by the seasonal uncertainty or deficiency of RES which may degrade the network performance. To overcome this problem as well as avoid power outage or power shortage, the integration of different energy sources is preferable. Combined installation of different RES such as hybrid PV/wind

turbine (WT), PV/biomass generator (BG), WT/BG, etc. mainly depends on the locally available RES and thus helps to enhance the network reliability. Additionally, EE of the integrated supply system can be improved by utilizing the renewable energy exchanging model among the neighboring BSs via the low resistive power line. Nowadays, modern cellular macro BSs are being installed with Radio Remote Head (RRH) which has the provision of reducing feeder loss by replacing the coaxial cable with the optical fiber link between the baseband and power amplifier. As a result, macrocell BS with RRH can save network energy consumption by increasing the EE without sacrificing QoS.

The organization of the rest of the paper is as follows: A throughout review of related work is discussed in Section II. Section III presents the system model for macrocell with RRH base station. Section III also highlights the mathematical modeling and description of the system components. Cost modeling and optimization formula are outlined in Section IV. The simulation setup considered in HOMER software and performance analysis are given in Section V. Additionally, a comparison between the proposed system and other systems is presented in Section V in terms of energy, economic and cleanliness issues. Finally, Section VI concludes the paper summarizing the key findings.

II. RELATED WORK

Recently, a lot of researches have been conducted where numerous methods have been proposed by the researchers to find out the long-term sustainable, reliable, energy-efficient and eco-friendly power supply for the next-generation cellular networks [33]–[35]. Some of them advocate for the combination of renewable energy sources with the traditional non-renewable energy sources while others consider the integration of different RE sources or a single RE source with a battery unit [36], [37]. Authors in [13], [22], [38] recommend a single renewable energy-focused solar PV system by addressing the challenges of implementing the solar PV powered BSs in off-grid sites. Chamola and Sikder [13] investigate the key challenges and propose some critical solutions for the installation and enhancement of solar PV enabled BSs. For ensuring a hundred percent energy autonomy and achieving long-term sustainability, a stand-alone solar-powered BS has been proposed by Alsharif [38]. The feasibility and sustainability of deploying green cellular networks have also been analyzed considering the solar radiation profile of South Korea in [22]. In these works, the optimal system architecture, capital cost and sustainability of the solar PV system have also been evaluated considering the yearly solar radiation profile. Although this work provides an excellent method of harvesting energy from the renewable energy source, the authors did not consider the effect of dynamic traffic and bandwidth variation.

Numerous authors investigate the sustainability and reliability of a combined power system for off-grid cellular BSs [7], [11], [39]. In remote areas, the concept of installing traditional only DG systems as a primary source is less favorable technology due to the higher fuel cost, operation & maintenance cost (OMC), pollution rate and low efficiency. However, it played a significant role in conjunction with RE sources [11], [23]. As a consequence, Huawei technology [24] has already developed a diesel power hybrid system in off-grid sites in Africa and the Middle East. Instead of using a conventional-only diesel generator system or a single PV system for harvesting energy, they [11], [39] advocated for a hybrid PV/DG (combination of green and fuel energy) for the reason of reducing the sole dependency on fossil fuel and increasing the reliability as compared to the single PV system. Though these works widely evaluate the technical issues and optimum modeling of a solar PV/DG system that secures the energy sustainability and reliability, the dynamic traffic pattern has not been discussed. The hybrid PV/DG system has many advantages over a single DG or single PV system but it partially contains some DG related difficulties such as high fuel cost, OMC and CO_2 emission. Authors in [40], investigate the potential of hybrid solar PV and PEM fuel cells system for powering the remote off-grid base stations. Reference [41], proposed a renewable hydrogen-based supply system. Reference [27], introduced a solar PV and biomass gasifier focused energy supply. Ani and Nzeako *et al.* in [42], discussed the optimization of a hybrid (Solar & Hydro) and DG powered scheme for a remote BS. In order to reduce the NPC, operational expenditures (OPEX) and greenhouse gas emission, authors in [43]–[45] mentioned a hybrid PV/WT system by integrating two renewable energy sources. Authors in [43], [44] explored the various key factors including the optimal sizing, net present cost and greenhouse gas contents for assessing the system performance. Nevertheless, authors have not examined the sustainability of the designed system by considering the variation of bandwidth and BS transmission power. Generating energy from wind requires sufficient wind speed which is usually available in coastal areas and offshore islands.

Combined utilization of different green energy sources along with the conventional grid supply has been extensively studied for achieving long term sustainable, and energy-efficient cellular networks [46]–[49]. Authors in [46]–[48] introduce both renewable energy and utility grid-supplied modern cellular networks adopting the different types of coordinated multipoint (CoMP) transmission techniques such as dynamic point selection and joint transmission. In these papers, the key challenges of utilizing the maximum amount of renewable energy reducing the grid energy consumption are critically analyzed considering the dynamic traffic pattern. Moreover, an extensive simulation is applied using MATLAB for evaluating the system performance under different parameters. Reference [49] evaluated the optimization of grid power consumption for hybrid renewable energy and the grid powered heterogeneous cellular networks (HetNets). The prime concern of this work is to reduce the grid power cost by controlling the transmitted power and stored energy in the context of coverage probability constraint. This innovative method can overcome the drawback of using

renewable energy and thus will help to improve energy efficiency ensuring QoS in the areas where the electrical power line is available.

Energy sustainability and OPEX saving of a cellular network can be achieved by improving the energy efficiency and by establishing a dynamic traffic management network as reported in [50]. In this way, a great amount of electricity can be saved by introducing a higher energy-efficient component along with the guaranteed quality of services. According to [51]–[53], transferring electricity among the neighboring base stations through a smart grid (SG) or low resistive line is a beneficial technique for increasing the EE of BSs. Farooq *et al.* [51] developed a combined green energy sharing technique, where the physical power line is used to share energy among the BSs. They have also used SG infrastructure to share the locally produced power. A framework of exchanging electricity between the two BSs via a low resistive conductor has been analyzed in [52]. Energy procurement within the BSs through SG is introduced in [54]. In order to improve the EE, the infrastructure sharing method has been mentioned in [55], [56], where the same radio access network (RAN) will be shared by the multiple network operators. Dynamic traffic management network adapts the transceivers transmission power based on the traffic density and particular element of the network such as power amplifier (PA) unit, radio frequency (RF) unit, and baseband (BB) unit. Even the entire BSs can be switched off during the low traffic density [50]. If the traffic density is high, this method cannot be executed. In this case, a certain number of BSs must always be in an active position in order to support the basic operation of the network [4].

A. CONTRIBUTIONS

Being inspired by the above analyses, this paper investigates the potential of solar PV and biomass resource-based hybrid power supply of macrocell BSs with RRH. This system can reduce the inconvenience that arises for using non-renewable energy sources. In this paper, the selected off-grid site is Saldanga union Parishad of Debiganj Upazila under the Panchagarh district in the Rangpur Division. The proposed framework introduces the process of harvesting renewable energy from solar and biomass resources with a set of battery bank because the output power of the renewable energy sources may be intermittent, and seasonal. Incorporated energy sharing technique with the combined configuration of solar PV, biomass and battery units can significantly increase energy efficiency. A comprehensive simulation using HOMER software has been done over 20 years' project duration to calculate the system performance considering the real traffic by varying the solar radiation and bandwidth under different transmission power. Additionally, MATLAB based simulation has been carried out to assess the system performance. The main contributions of this paper can be summarized as follow:

- To determine the optimal system configuration and technical criteria of the solar PV and biomass resources based hybrid supply system to provide power to the off-grid LTE cellular BSs.
- To evaluate and assess the feasibility of the proposed hybrid system in terms of energy yield, carbon footprints, economic aspects, throughput, and energy efficiency which ensure the long term sustainability with guaranteed quality of services.
- To increase network performance and save energy by utilizing green energy sharing techniques among the neighboring BSs via a low resistive power line.
- To compare the outcomes of the proposed system with the stand-alone solar PV and hybrid PV/DG system in terms of techno-economic factors and greenhouse gas emissions.

III. SYSTEM MODEL

Fig. 1 exhibits the architecture of the hybrid solar PV/biomass system which integrates two different renewable energy sources in order to ensure the reliable, sustainable and clean electricity supply to the macrocell BS in LTE cellular network. A short description of the major components of the proposed model and the corresponding mathematical modeling are provided below:

A. NETWORK MODEL

In this network, a macro base station with a 2/2/2 antenna pattern in hexagonal shape has been considered which acts as an access link between the mobile station and core network. A typical BS consists of different types of power-consuming equipment such as digital signal processing or baseband unit (BB), transceiver (TRX) unit, radio frequency (RF) unit, power amplifier (PA) unit, and DC-DC regulator. The proposed network model is a combination of renewable energy harvester (solar & biomass), BS, converter, battery bank, and a smart energy management unit (EMU). The BS is generally a DC load. It also includes some AC loads as auxiliary equipment such as air conditioning and lighting. In this model, we consider only one 30 W AC lamp which is connected to the BS from 6 PM to 6 AM. Macro BS with RRH does not require any cooling arrangement. An EMU act as a charge controller by protecting the overvoltage and preventing the deep charging of the storage device. It is widely recognized that a 2/2/2 LTE macro BS operates at 20W (43dBm) and 40W (46dBm) [57]. However, 20W transmit power is broadly used. The term 2/2/2 represents that a BS includes three sectors with each sector having two antennas.

The algorithm of the introduced system is simplified in a flowchart as demonstrated in Fig. 2. The operation of the network can be divided into the following three states: Firstly, energy is supplied to the BS by the hybrid solar PV/biomass scheme where excess electricity is stored in the battery bank. Secondly, if the solar PV/biomass energy is not sufficient due to the deficiency of solar/biomass resources or seasonal change, the storage device will provide backup electricity. It is to be mentioned that the storage device can autonomously

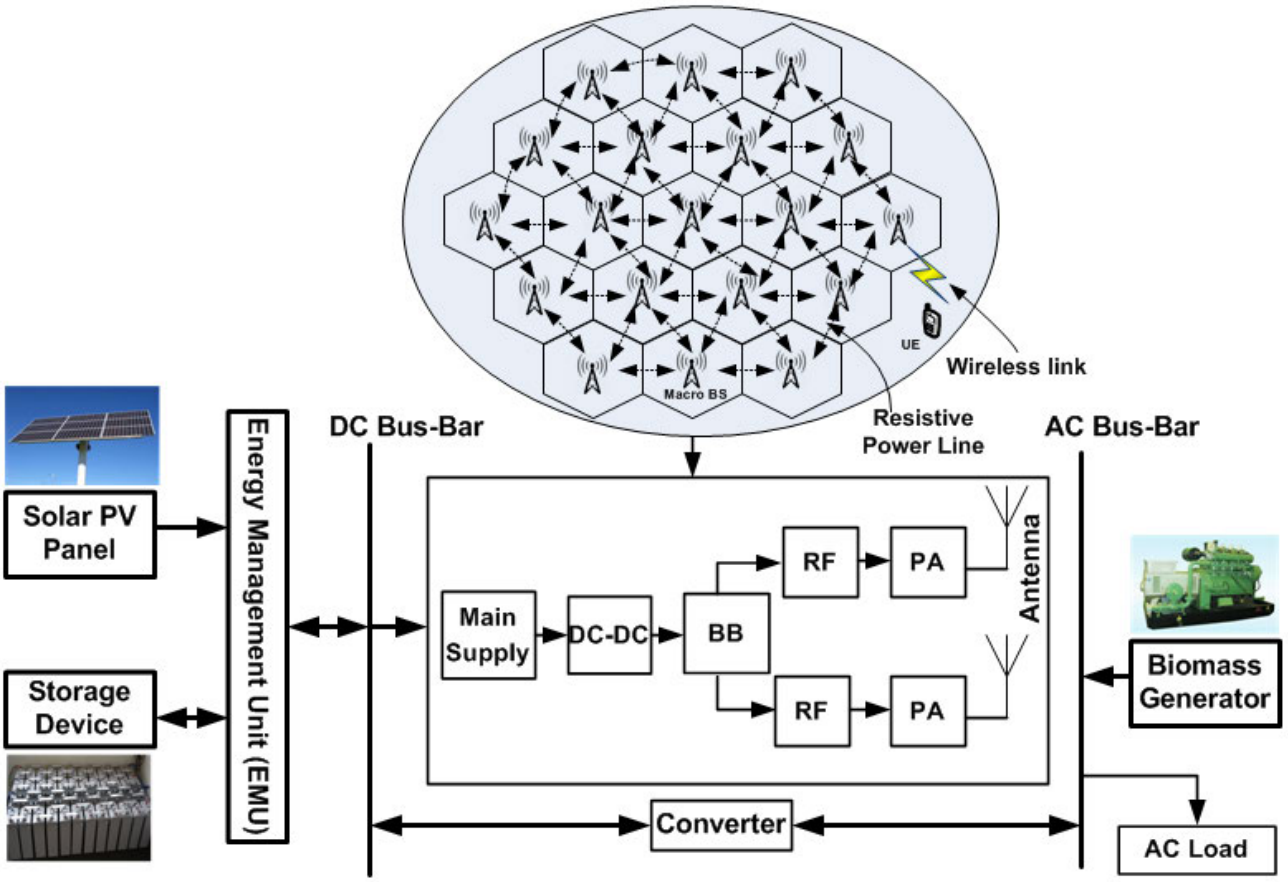

FIGURE 1. Architecture of the proposed hybrid solar PV/BG system.

support the BS around 6.75 days and 4.5 days respectively for $P_{TX} = 20$W and $P_{TX} = 40$W. This support continues till it reaches the minimum depth of discharge which is sufficient time to fix the hybrid system. Thirdly, it will share the energy to the neighboring needy BS if the excess electricity is greater than the threshold level (10% of load requirement). It will also receive energy from the nearest BS in case of an energy shortage via a low resistive power line. This sharing technique is aimed at the maximum utilization of renewable energy sources without scarifying their own energy demand.

B. SOLAR PV PANEL

Solar is the most available, clean and enormous renewable source of energy throughout the world. The solar PV panel collects solar energy and converts it into electrical energy. Several solar PV cells are connected in series/parallel to form a solar PV array for harvesting more energy. Total renewable energy harvested by the solar PV panel can be found by (1) [43]

$$E_{PV} = R_{PV} \times PSH \times \eta_{PV} \times 365 days/year, \quad (1)$$

where R_{PV} is the rated capacity of the solar PV panel in kW. PSH is a peak solar hour in an hour which is equivalent to average daily sunlight intensity in $kWh/m^2/day$. η_{PV} is the derating factor which refers to the efficiency of the solar PV panel. The output power of the solar PV panels mostly depends on the solar radiation profile, geographical location, DC-DC loss factor, tracking mode and the tilt of the solar PV panel [43]. Moreover, an Internet of Things (IoT) based sun tracking system increases the generated energy [58].

The required number of solar PV panel (N_{PV}) to produce a specific output (P_p) can be formulated as follows [45]

$$N_{PV} = \frac{P_p}{P_{max}}, \quad (2)$$

where P_{max} is the maximum power of the solar PV panel. Table 1 represents the specification of the considered solar PV panel.

Fig. 3 represents the temporal variation of daily solar energy production by 1 kW solar PV panel, which is calculated with the help of the System Advisory Model (SAM). Fig. 4 depicts the average yearly solar energy generation for a given location in Bangladesh. The average value of sunlight intensity varies from one place to another; the highest sunlight intensity is 5.48 $kWh/m^2/day$ in April and the lowest intensity is 3.78 $kWh/m^2/day$ in July.

However, there are some difficulties and challenges of energy generation by the solar cell due to the dirt, dust, tree

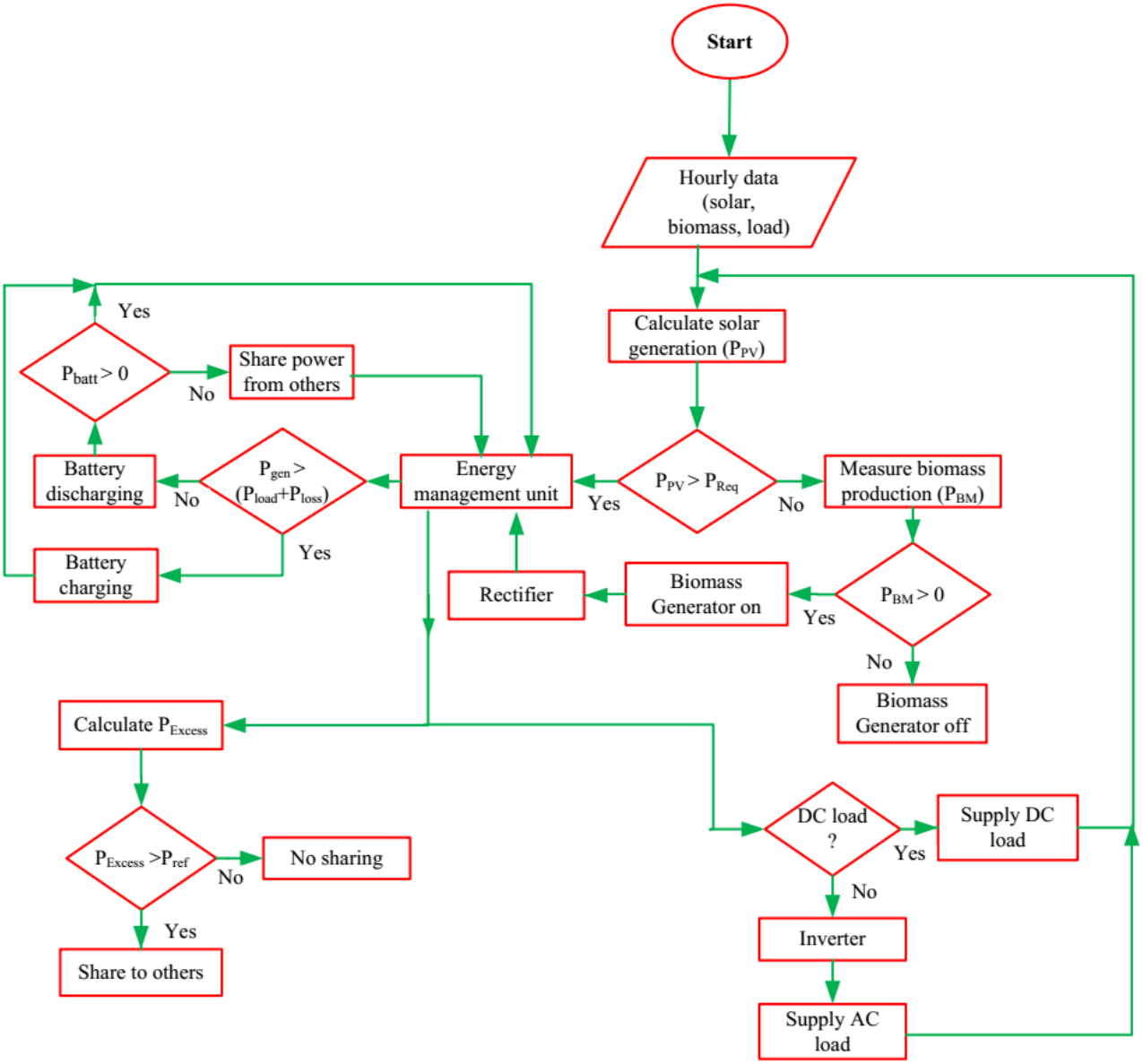

FIGURE 2. Flow chart of the proposed hybrid solar PV/BG system.

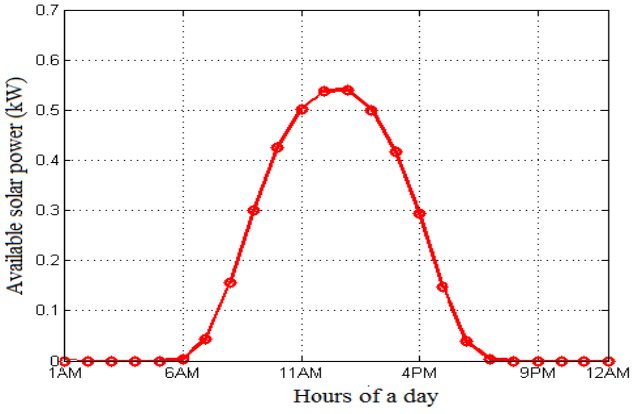

FIGURE 3. Average hourly solar power production over a day.

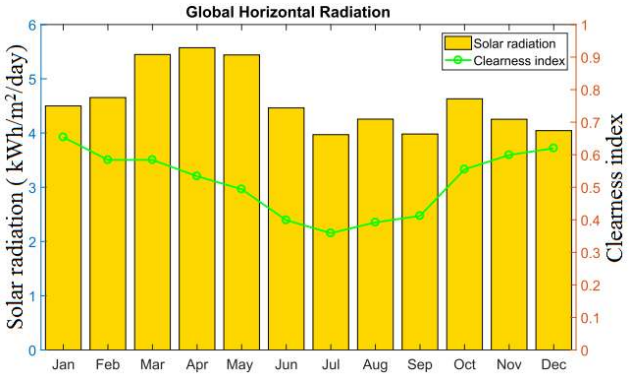

FIGURE 4. Average yarly solar radiation profile in Bangladesh.

debris, water spots, mould, tree shade, fog, cloud and heavy rain in the tropical country. To overcome these problems, the hybridization of solar energy with biomass energy in remote areas can be a promising solution.

TABLE 1. Specifications of the solar PV panel [45].

Parameters	Type (Value)
Solar module type	Sharp ND-250QCs (poly crystalline)
Nominal voltage (V)	29.80 V_{DC}
Nominal current (A)	8.40 Amp
Maximum power (P_{max})	250 $Watt$
Cell Configuration	60 in series
Open circuit voltage (V_{oc})	38.3 V_{DC}
Short circuit current (I_{sc})	8.90 Amp

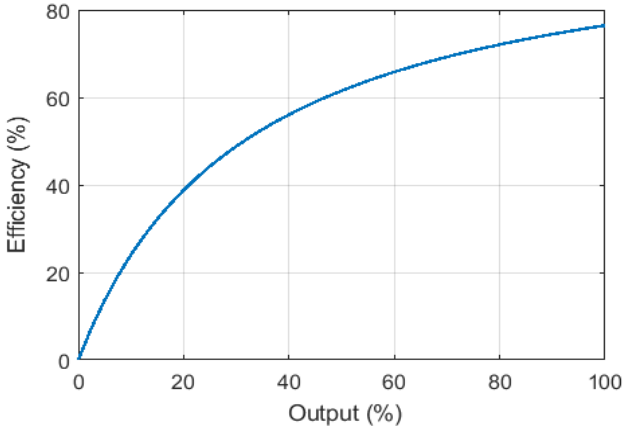

FIGURE 5. Characteristic curve of the biomass generator.

C. BIOMASS GENERATOR

At present, energy harvesting from the biomass has become a mature technology and in our country, most of the available biomass resources are agriculture residue, animal dung, poultry dropping, etc. [20]. Moreover, as an agricultural country (over 60% production comes from fertile land), Bangladesh has enough potential for renewable energy harvesting from agricultural residue particularly from the rice husk and crop residue. Out of the agriculture residue, rice husk is a powdy/fine biomass whose average calorific value is around 14274 KJ/Kg (3411.33 KCal/Kg). Theoretically, one-ton paddy can produce around 200 Kg rice husk but practically, the average amount is expected 187 Kg [27]. Additionally, 1.5-4 Kg/hr rice husk is required to produce 1 kWh energy. In this simulation, the maximum collection capacity of rice husk is considered around 20% (9 tons/day) of total rice husk available in the area and the cost of biomass is taken as $30/tons [27].

The parameters of the biomass generator are provided in Table 5 and its characteristic curve is presented in Fig. 5. Power production from the biomass generator system depends on the various factors such as the calorific value of biomass (CV_{BM}), availability of biomass (T_{BM}), an operating hour of the biomass generator per day (t_{op}) and overall efficiency of biomass conversion process (n_{BM}) which can be expressed as follows [20], [27]

$$P_{BG} = \frac{T_{BM}(tons/year) \times CV_{BM} \times \eta_{BM} \times 1000}{365 \times 860 \times t_{op}}. \quad (3)$$

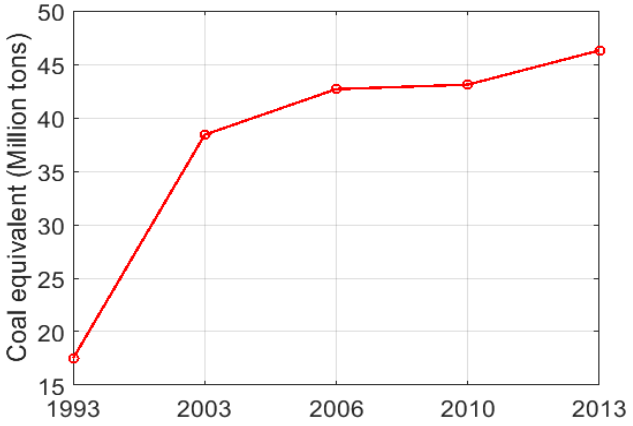

FIGURE 6. Biomass energy potential in Bangladesh.

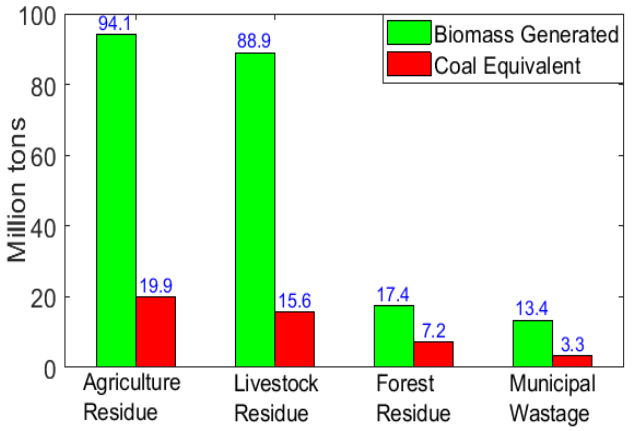

FIGURE 7. Biomass energy potential from different sources in Bangladesh.

Yearly energy generated by the biomass generator can be calculated as [20], [27]

$$E_{BG} = P_{BG}(365 \times 24 \times capacity \quad factor), \quad (4)$$

where the capacity factor is the ratio of actual electrical energy output to the maximum possible electrical energy output over a given period of time. In this work, the set capacity factor is 0.26.

In 2003, Bangladesh had around 74.128 million tons of biomass which are equivalent to 38.41 million tons of coal [26]. Fig. 6 depicts the yearly increasing coal equivalent biomass energy potential in Bangladesh. Additionally, Fig. 7 illustrates the biomass energy potential from different sources in Bangladesh [25].

D. DIESEL GENERATOR

The integration of DG with renewable energy sources plays a significant role in compensating the capital cost and BS energy demand during RES malfunction. This subsection represents the mathematical model of DG in order to compare the result of the suggested hybrid PV/BG system with the hybrid PV/DG system. Energy generated by a DG (E_{DG}) in kWh with rated power output (P_{DG}) can be determined as

follows

$$E_{DG} = P_{DG} \times \eta_{DG} \times t_{op}, \tag{5}$$

where η_{DG} is the efficiency of the DG and t_{op} is the operational time. However, the fuel consumption (F_C) is calculated by

$$F_C = E_{DG} \times f_{sp}, \tag{6}$$

where f_{sp} is the specific fuel consumption (L/kWh). Generally, a DG set emits carbon footprint of 2.68kg/L [11].

E. CONVERTER

When a system is compatible with both AC and DC loads a converter is required to obtain the desired frequency and uninterruptible power supply to the load with high efficiency. A converter can act as an inverter, rectifier, or both of them. Depending on the output power, output voltage and installation type inverter may be different and the capacity of the inverter can be determined by [11]

$$C_{inv} = (\frac{L_{AC}}{\eta_{inv}}) \times \sigma_{sf}, \tag{7}$$

where L_{AC} is the maximum AC load in kW, η_{inv} is the efficiency of the inverter, and σ_{sf} is the safety factor. The efficiency of the inverter can be determined as follows [59]

$$\eta_{inv} = \frac{P}{P + P_0 + KP^2}. \tag{8}$$

The value of P, P_o, and K can be calculated respectively by (9), (10) and (11) [59]

$$P = \frac{P_{out}}{P_{in}}, \tag{9}$$

$$P_0 = 1 - 99\frac{10}{\eta_{10}} - \frac{1}{\eta_{100}} - 9, \tag{10}$$

$$K = 1 - \frac{1}{\eta_{100}} - P_0 - 1, \tag{11}$$

where P is the efficiency of the inverter at its rated power. On the other hand, η_{10} and η_{100} represent the inverter efficiency respectively at 10% and 100% of its nominal power supplied by the manufacturers.

F. BATTERY BANK

The battery bank is a backup device that acts as an energy buffer by compensating the mismatch between the energy generation and the demand. On focusing the capital cost, and characteristics 'Trojan L16P' battery model is considered in this work. Additional information can be found in 'www.trojanbattery.com'.

The depth of discharge (B_{DOD}) is an important characteristic for selecting the battery bank capacity that tells how deeply the battery is discharged along with the battery state of charge (SOC). Battery state of charge is the indicator of the charging and discharging level of the battery which is expressed in percentage. The maximum state of charge (SOC_{max}) represents the nominal capacity of the battery bank and minimum state of charge (SOC_{min}) represents the lower limit of battery discharge. The B_{DOD} of Trojan L16P battery is 70% which implies that 70% of its energy has been delivered and 30% energy is reserved. The B_{DOD} can be calculated as follows [45]

$$B_{DOD} = (1 - \frac{B_{SOC_{min}}}{100}). \tag{12}$$

The backup time of the storage device is directly related to the capacity of the battery and can be expressed as [45]

$$B_c = \frac{P_{BS} \times D \times t_w}{B_{DOD} \times V_b \times K_b}, \tag{13}$$

where P_{BS} is the BS DC load in W, D is the backup time, t_w is the load working time, V_b is the battery voltage compatible at 48 V DC bus bar and K_b (1.14) is the battery capacity coefficient.

The storage capacity of the battery bank is a function of the number of batteries (N_{batt}), the nominal voltage of each battery (V_{nom}), nominal capacity of a single battery (Q_{nom}), and battery state of charge (B_{SOC}) that can be determined as follows [45]

$$E_{battmax} = \frac{N_{batt} \times V_{nom} \times Q_{nom}}{1000} \times B_{SOC\,max}, \tag{14}$$

$$E_{battmin} = \frac{N_{batt} \times V_{nom} \times Q_{nom}}{1000} \times B_{SOC\,min}, \tag{15}$$

$E_{battmax}$ and $E_{battmin}$ denote the maximum and minimum storage capacity of the battery bank in kWh.

Battery bank autonomy (B_{aut}) illustrates the number of hours that the fully charged batteries can back up the load without any support from the external power source. B_{aut} can be defined as the ratio of battery bank size to the BS electrical load and is determined in HOMER by the following equation [45]

$$B_{aut} = \frac{N_{batt} \times V_{nom} \times Q_{nom} \times B_{DOD} \times (24h/day)}{L_{BS}}, \tag{16}$$

where L_{BS} average daily BS load in kWh.

Battery lifetime (L_{batt}) mainly depends on two factors: battery float life and lifetime throughput. In other words, batteries die either from the use or from the old age. Battery lifetime plays a significant role in order to minimize the total replacement cost within the project duration. Based on these two factors, the overall lifetime of a battery can be determined as follows [45]

$$L_{batt} = min(\frac{N_{batt} \times Q_{life}}{Q_{tp}}, B_f), \tag{17}$$

where Q_{life} is the lifetime throughput of a single battery in kWh, Q_{tp} is the annual battery throughput (kWh) and B_f is the battery float life in years. Throughput is defined as the change in the energy level of the battery bank, measured after charging losses and before discharging losses. Lifetime throughput is the amount of energy that can be cycled through the battery bank before it dies and annual throughput is the amount of energy that cycles through the battery per year. The float life of the battery is the maximum length of time that

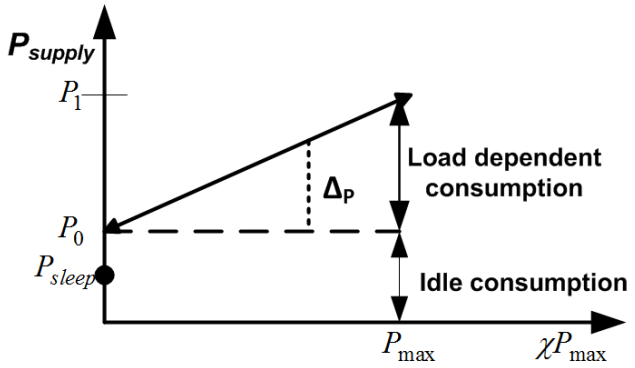

FIGURE 8. BS power consumption.

the battery will last before it needs replacement, regardless of how much or how little it is used.

The number of batteries connected in series (N_{batt}^{series}) and connected in parallel ($N_{batt}^{parallel}$) can be found by the following equation [45]

$$N_{batt}^{series} = \frac{V_{bb}}{V_{nom}}, \tag{18}$$

$$N_{batt}^{parallel} = \frac{N_{total}}{N_{batt}^{series}}, \tag{19}$$

where V_{bb} is the DC bus-bar voltage and V_{nom} is the nominal voltage of the battery.

G. BS POWER PROFILE

In order to determine the dimension and analyze the performance of the hybrid PV/biomass system, it is very momentous to assess the energy consumption of the BS considering the incoming traffic rate. The power consumption of a typical BS is dynamic in nature and mostly depends on the traffic profile of the BS, which varies over time and space. As refer to the [60], the power consumption of a BS can be expressed as an affine function of the transmission power. In other words, the consumption contains a load-independent static power P_0 and load-dependent linearly raising power P_1 as displayed in Fig. 8. Additionally, Fig. 9 illustrates the base station traffic profile which is approximated by using the Poisson distribution model and can be expressed as follows [45]

$$\lambda(t) = \frac{p(t,\alpha)}{max[p(t,\alpha)]}, \tag{20}$$

$$p(t,\alpha) = \frac{\alpha^t}{t!}e^{-\alpha}, \tag{21}$$

where $\lambda(t)$ is the normalized traffic distribution, $p(t,\alpha)$ is the Poisson distribution function of traffic demand at a particular point of time, and α is the mean value.

The total power consumption of a BS as a function of traffic intensity is shown in Fig. 9 and can be represented as follows [61]

$$P_{in} = \begin{cases} N_{TRX}[P_1 + \Delta_p P_{TX}(\chi - 1)], & \text{if } 0 < \chi \leq 1, \\ N_{TRX}P_{sleep}, & \text{if } \chi = 0, \end{cases} \tag{22}$$

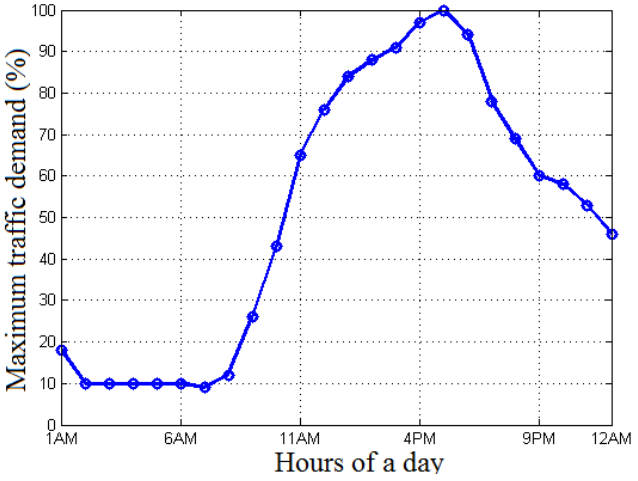

FIGURE 9. Dynamic traffic profile over a day.

TABLE 2. Base station key parameters [61].

Macro BS	N_{TRX}	$P_{TX}[W]$	$P_0[W]$	Δ_P	$P_{sleep}[W]$
w/o RRH	6	20 and 40	130	4.7	75
with RRH	6	20 and 40	84	2.8	56

where $P_1 = P_0 + \Delta_p P_{TX}$ is the height of power consumption of a BS, N_{TRX} is the total number of the transceiver, Δ_p is the load dependency power gradient and P_0 is the consumption at idle state [61]. The scaling parameter χ is the load share, where $\chi = 1$ indicates that a fully loaded system and $\chi = 0$ indicates an idle system. Furthermore, a BS without any traffic load enters into sleep mode with lowered consumption, P_{sleep}. Table 2 represents the key parameters of a BS.

The power consumption of each individual element of the macrocell with RRH for both $P_{TX} = 20$W and $P_{TX} = 40$W is summarised in Table 3. Power losses in BSs primarily occur in the DC-DC regulator, main supply, and active cooling system which are linearly rising with the power consumption of the other component. These three aspects are respectively symbolized by σ_{DC}, σ_{cool} and σ_{MS}. The active cooling system is essential only for the macro BS. It is not necessary for the RRH and microcell type BS. In macrocell BS with RRH, the power amplifier (PA) is placed near the transmit antenna for saving power by eliminating feeder and active cooling losses. The maximum power consumption of a BS is determined as [61]

$$P_1 = \frac{P_{BB} + P_{RF} + P_{PA}}{(1 - \sigma_{DC})(1 - \sigma_{MS})(1 - \sigma_{cool})}, \tag{23}$$

where P_{BB}, P_{PA} and P_{RF} respectively refer to the baseband, power amplifier and RF power consumption for the given 10MHz transmission bandwidth as obtained from Table 3. The amount of power received by the power amplifier (P_{PA}) mainly depends on the maximum transmission power per antenna (P_{TX}), feeder losses (σ_{feed}) and the efficiency of the power amplifier (η_{PA}), which can be represented as follows

$$P_{PA} = \frac{P_{TX}}{\eta_{PA}(1 - \sigma_{feed})}, \tag{24}$$

TABLE 3. BS power breakdown under peak load for 10 MHz bandwidth [60].

Components	Parameters	with RRH
Base station (BS)	Type	Macro
	P_{TX} [W]	20
	Feeder loss σ_{feed} [dB]	0
Power amplifier (PA)	Back-off [dB]	8
	Max PA out [dBm]	51
	PA efficiency η_{PA} [%]	31.1
	Total PA, $\frac{P_{TX}}{\eta_{PA}(1-\sigma_{feed})}$ [W]	64.4
Radio frequency (RF)	P_{TX} [W]	6.8
	P_{RX} [W]	6.1
	Total RF, P_{RF} [W]	12.9
Baseband (BB)	Radio (inner Tx/Rx) [W]	10.8
	Turbo code(outer Tx/Rx) [W]	8.8
	Processors [W]	10
	Total BB, P_{BB} [W]	29.6
DC-DC	σ_{DC} [%]	7.5
Cooling	σ_{cool} [%]	0
Mains Supply	σ_{MS} [%]	9
Sectors		3
Antennas		2
Total power [W]		**754.8**

where the efficiency and loss factor can be defined as:

$$\eta = \frac{P_{out}}{P_{in}}$$

and

$$\sigma = 1 - \eta.$$

The power consumption by the baseband and radio frequency linearly varies with the bandwidth (BW) and a number of transceiver antenna (D) while the other parameters remain the same. The power consumption can be expressed as follows [61]

$$P'_{BB} = N_{TRX}\frac{BW}{10MHz}P_{BB}, \tag{25}$$

$$P'_{RF} = N_{TRX}\frac{BW}{10MHz}P_{RF}, \tag{26}$$

where P'_{BB} and P'_{RF} are respectively the baseband and RF power consumption for the desired bandwidth.

H. POWER AND ENERGY MODEL

The term 'annual capacity shortage' (R_{CS}) is an indicator of power reliability and is explained as the ratio of annual energy deficiency (E_{CS}) to the annual BS load demand (E_{BS}) [45].

$$R_{CS} = \frac{E_{CS}}{E_{BS}}, \tag{27}$$

where E_{BS} is expressed in kWh/yr and E_{CS} can be represented as follows

$$E_{CS} = E_{BS} - E_{gen}, \tag{28}$$

where E_{gen} is the generated electricity which can be written as

$$E_{gen} = E_{PV} + E_{BG}. \tag{29}$$

A reliable system can be developed by fulfilling the base station demand with sufficient backup power over the entire project duration. For the suggested hybrid PV/BG scheme, excess electricity (E_{Excess}) can be generated when total energy generation is over than the base station energy requirement that can be formulated by the following equation

$$E_{Excess} = E_{gen} - E_{BS} - C_{loss} - B_{loss}, \tag{30}$$

where C_{loss} and B_{loss} respectively represent the losses associated with converter and battery.

I. ENERGY SHARING MODEL

While a BS contains the required level of excess electricity (10% of load), it can exchange the energy to the neighboring BS having a shortage of energy. It also indicates that a BS can get green energy support from the adjacent BSs via a low resistive path for maintaining the continuous services for its users. The amount of shared electricity (E_{share}) can be expressed as

$$E_{share} = E_{Excess} - E_{loss}, \tag{31}$$

where E_{loss} is the amount of energy loss in the transmission line during the period (t_r) which can be calculated as follows [45]

$$E_{loss} = I^2R(l) \times t_r = \frac{P^2_{share}R(l)}{V^2} \times t_r, \tag{32}$$

where I is the current flowing through the transmission line, R is the ohmic value of the entire line, V is the DC 48 volt, and P_{share} is the shared power. Total shared energy and average energy saved by the sharing mechanism can be determined as follows [45]

$$E_{share} = P_{share} \times t_{op}, \tag{33}$$

$$E_{saving} = \frac{\sum_{i=1}^{N} E_{share}(t)}{\sum_{i=1}^{N} E_{BS}(t)} \times 100\%, \tag{34}$$

where N is the number of sharing BS, typically 19 for the two-tier configuration as shown in Fig. 1 and E_{BS} is the required energy of i^{th} BS. Green energy sharing is an effective tool for ensuring zero power outage of remote off-grid cellular BSs, which enhance the system reliability and sustainability.

J. ENERGY EFFICIENCY MODEL

In this work, a shadow fading channel model with log-normally distributed has been considered. Path loss is calculated in dB for the interval of d between the transmitter and receiver. Path loss can be defined as follows [14]

$$PL(d) = PL(d_0) + 10\alpha log_{10}\left(\frac{d}{d_0}\right) + X_\sigma, \tag{35}$$

where $PL(d_0)$ is the path loss for the reference distance (d_0), α is the exponent of path loss. Path loss for reference distance can be evaluated from the free-space path loss equation.

For k^{th} user equipment (UE), the received power at a distance $d = d^{i,k}$ from i^{th} BS β_i is given by [14]

$$P^{i,k}_{rx} = P^{i,k}_{tx} - PL(d) + X_\sigma, \tag{36}$$

where $P_{tx}^{i,k}$ is the transmitted power in dBm and X_σ is the amount of shadow fading modeled as a zero-mean Gaussian random variable with a standard deviation σ dB. The transmit power $P_{tx}^{i,k}$ from BS i to UE k satisfies $\sum_{k\epsilon U} P_{tx}^{i,k} \leq P_i^{max}$, where P_i^{max} is RF output power of BS β_i at its maximum traffic load and U is the number of active UE in this BS.

The inter-cell interference (ICI), $P_{k,inter}$, can be determined by [14]

$$P_{k,inter} = \sum_{m \neq i} (P_{rx}^{m,k}). \tag{37}$$

Then, the received signal to interference plus noise ratio (SINR) at k_{th} UE from BS β_i can be given by [14]

$$SINR_{i,k} = \frac{P_{rx}^{i,k}}{P_{k,inter} + P_{k,intra} + P_N}, \tag{38}$$

where $P_{k,intra}$ is the intra-cell interference, P_N is the additive white Gaussian noise (AWGN) power given by $P_N = -174 + 10log_{10}(BW)$ in dBm with BW is the bandwidth in Hz. Notwithstanding, orthogonal frequency division multiple access (OFDMA) technique in the LTE system includes zero ICI.

Energy efficiency (EE) is used to measure the performance and can be denoted as the number of bits transmitted per Joule of energy. According to Shanon's information capacity theorem, total achievable throughput in a network at time t can be approximated as follows [14]

$$C_{total}(t) = \sum_{k=1}^{U} \sum_{i=1}^{N} BWlog_2(1 + SINR_{i,k}), \tag{39}$$

where N and U represent the number of transmitting BSs and the total number of UEs in the network. Hence, the EE metric (N_{EE}) of a network can be expressed as follows [14]

$$N_{EE} = \frac{C_{total}}{P_{net}}, \tag{40}$$

where P_{net} is the total power consumed in all the BSs at time t and can be calculated by using (22).

The throughput and energy efficiency performance of the proposed networks are performed with the help of MATLAB software, which is commonly known as Monte-Carlo simulation. The simulations are executed by averaging above ten thousand iterations considering the dynamic traffic pattern. We also assumed that every user is linked with one resource block (RB). The basic parameters of the simulation setup are summarized in Table 4.

TABLE 4. Key parameters for MATLAB based Monte-Carlo simulation setup [14].

Parameters	Value
Resource block (RB) bandwidth	180 kHz
System bandwidth, BW	5,10,15,20 MHz
Carrier frequency, f_c	2 GHz
Duplex mode	FFD
Cell radius	1000 m
BS Transmission power	46 dBm
Noise power density	-174 dBm/Hz
Number of sectors	3
Number of antennas	2
Reference distance, d_0	100 m
Path loss exponent, α	3.574
Shadow fading, X_σ	8 dB
Access technique, DL	OFDMA
Traffic model	Randomly distributed

IV. COST MODELING AND OPTIMIZATION FORMULA

HOMER determines various types of costs associated with the project such as capital cost (CC), replacement cost (RC), net present cost (NPC), cost of electricity (COE), operation & maintenance cost (OMC), and salvage value (SV). The economic feasibility of the proposed model can be evaluated with the help of these costs. The NPC of the system can be formulated as follows [45]

$$NPC = \frac{TAC}{CRF} = CC + RC + OMC - SV. \tag{41}$$

The terms TAC and CRF respectively represent the total annualized cost and capital recovery factor of the system, which can be determined by (42) and (43) [45]

$$TAC = TAC_{CC} + TAC_{RC} + TAC_{OMC}, \tag{42}$$

$$CRF = \frac{i(1+i)^N}{(1+i)^N - 1}, \tag{43}$$

where N is the project lifetime and i is the annual real interest rate.

The cost remaining at the end of the project is known as salvage value which is evaluated by

$$SV = C_{rep}(\frac{R_{rem}}{R_{comp}}), \tag{44}$$

where C_{rep} is the replacement cost of the component, R_{rem} is the remaining lifetime of the component, and R_{comp} is the lifetime of the component.

The involvement of biomass and diesel generator includes a significant amount of fuel cost (FC). As a consequence, NPC of the BG and DG enabled system can be computed as follows

$$NPC = CC + RC + OMC + FC - SV. \tag{45}$$

Cost of electricity (COE) is defined as the ratio of the total annualized cost (TAC) to the annual electricity production (E_{gen}) by the system [45]. COE also measures the cost of unit electricity produced which can be represented as $\$/kWh$.

$$COE = \frac{TAC}{E_{gen}} = \frac{NPC \times CRF}{E_{gen}}. \tag{46}$$

The hybrid energy system design problem is formulated as an optimization problem with the objective function of minimizing NPC subject to various design and operational constraints. In other words, our prime goal is to minimize the energy shortage through maximum utilization of solar and biomass energy in conjunction with a battery bank which in turn reduces NPC [45]. The objective function of the system can be expressed as

$$\text{minimize } NPC, \tag{47a}$$

$$\text{subject to } E_{PV} + E_{BG} > E_{BS} \tag{47b}$$

TABLE 5. Key parameters and their specifications for HOMER simulation setup [25], [43].

System Components	Parameters	Value
Resources	Solar radiation	4.59 kWh/m^2/day
	Biomass available	9 tons/day
	Interest rate	6.75%
Solar PV	Operational lifetime	25 years
	Derating factor	0.9
	System tracking	Dual-axis
	Capital cost	$1/W
	Replacement cost	$1/W
	OMC/year	$0.01/W
Biomass Generator (BG)	Efficiency	30%
	Operational lifetime	25,000 h
	Capital cost	$0.66/W
	Replacement cost	$0.66/W
	OMC/year	$0.05/h
	Fuel cost	$30/ton
Diesel Generator (DG)	Efficiency	40%
	Operational lifetime	25,000h
	Capital cost	$0.66/W
	Replacement cost	$0.66/W
	OMC/year	$0.05/h
Battery	Round trip efficiency	85%
	$B_{SoC_{min}}$	30%
	V_{nom}	6 V
	Q_{nom}	360 Ah
	Capital cost	$300/unit
	Replacement cost	$300/unit
	OMC/year	$10/unit
Converter	Efficiency	95%
	Operational lifetime	15 years
	Capital cost	$0.4/W
	Replacement cost	$0.4/W
	OMC/year	$0.01/W

$$E_{PV} + E_{BG} + E_{batt} = E_{BS} + E_{loss} \quad (47c)$$

$$E_{Excess} = E_{gen} - E_{BS} - E_{loss} \quad (47d)$$

$$E_{battmin} \leq E_{batt} \leq E_{battmax}, \quad (47e)$$

where E_{loss} is calculated in kWh/year involving both the converter losses (C_{loss}) and battery losses (B_{loss}). The combined energy contribution by solar PV panels and biomass generators can certainly meet the annual BS demand to ensure power reliability mentioned in (47b). The constraint in (47c) ensures that the annual energy obtained by the integrated renewable energy sources carries the annual BS consumption with its associated losses. The amount of excess electricity is preserved for future use as described by the constraint (47d). The reserved energy also satisfies the power reliability constraint. The constraint (47e) implies that the battery bank storage capacity should not exceed the maximum limit and not reach below the threshold level.

V. PERFORMANCE ANALYSIS

A. SYSTEM IMPLEMENTATION AND CONFIGURATION

The project lifetime and annual interest rate are the vital issues for evaluating the economic feasibility of the project, because of their direct effect on total project cost. In this simulation, the project duration is 20 years that represents the lifetime of the BS equipment and long term feasibility

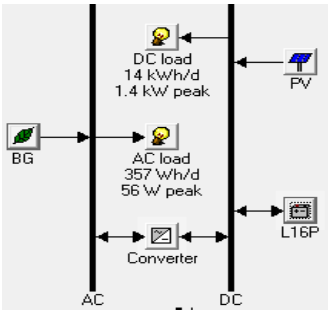

FIGURE 10. Schematic diagram in HOMER for macro BS under P_{TX} = 20W, and BW = 10MHz.

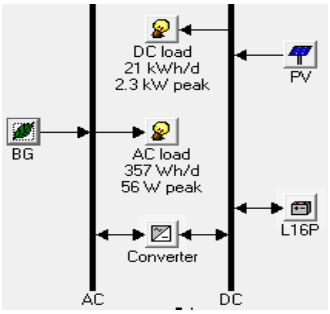

FIGURE 11. Schematic diagram in HOMER for macro BS under P_{TX} = 40W, and BW = 10MHz.

of the proposed system. The annual interest rate is 6.75%, which is the interest rate of Bangladesh bank. Energy shortage or outage is not acceptable in the telecom sector; thus, the sources must supply power to both the BS system and the backup system. As a consequence, 10% power is reserved for ensuring 0% annual capacity shortage and for providing backup power to the BS load under a certain decrease in the renewable energy output. Moreover, several sets of size, cost parameters of different components such as solar PV panel, biomass generator, converter, battery unit, and solar/biomass resource profile of the chosen area are set in HOMER software to find out the optimal criteria. HOMER is optimization software that makes a decision at each time step to satisfy the BSs load requirement that is related to traffic density and keep provision for backup power at the lowest NPC. The technical specifications, economic parameters, and system constraints that are used in this simulation setup are summarized in Table 5.

B. RESULTS AND DISCUSSION

The optimal system architecture, energy yield analysis, energy efficiency analysis, cost analysis, and greenhouse gas emissions of the solar PV/biomass system are provided in this section.

1) OPTIMAL SYSTEM ARCHITECTURE

Fig. 10 and 11 represent the HOMER schematic diagram for the proposed network under 10MHz bandwidth. Additionally, Fig. 12 and 13 depict the seasonal DC load profile of macro BS respectively for P_{TX} = 20W and P_{TX} = 40W.

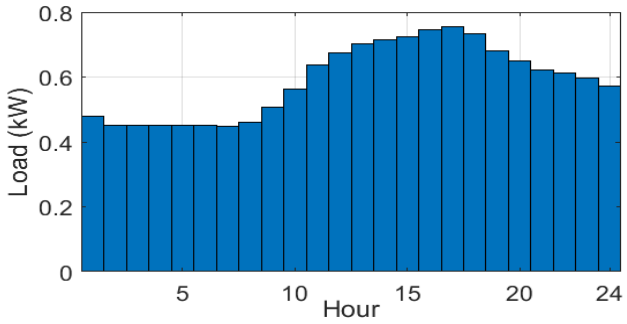

FIGURE 12. Seasonal DC load profile in HOMER for macro BS under P_{TX} = 20W, and BW = 10MHz.

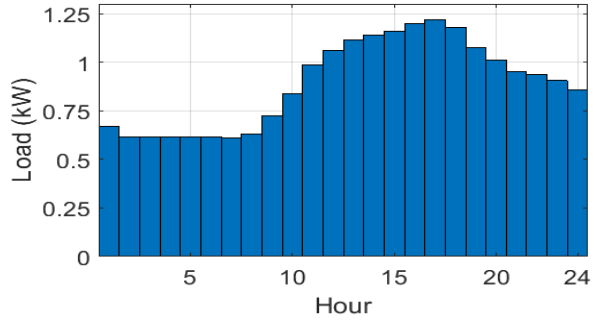

FIGURE 13. Seasonal DC load profile in HOMER for macro BS under P_{TX} = 40W, and BW = 10MHz.

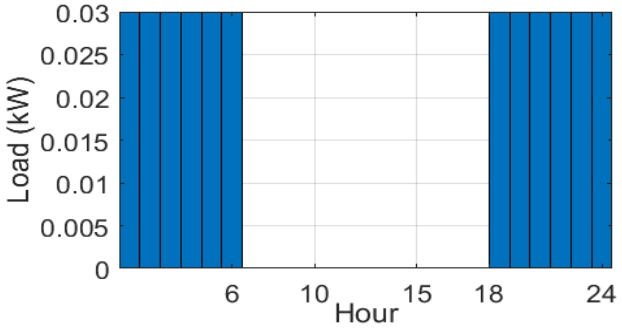

FIGURE 14. Seasonal AC load profile in HOMER for both P_{TX} = 20W, and P_{TX} = 40W under 10MHz BW.

Based on the load profiles, HOMER determined the optimal size of the different components considering solar radiation of 4.59 $kWh/m^2/day$ and 9 tons/day of biomass. On the other hand, the AC load profile under the same network setting for both transmission power is shown in Fig. 14. To increase the coverage area and QoS, a higher P_{TX} is required which uplifts the base station DC load as well as BS total energy demand.

Table 6 includes a summary of the technical criteria for designing the optimal system architecture and Table 7 illustrates the optimal size of the different components for 10MHz bandwidth under diverse solar radiation. It is clearly seen that the optimal size of the solar PV panel is inversely proportional to the solar intensity except for the radiation of 4 $kWh/m^2/day$. It is happening because a higher value of solar intensity produces higher energy with smaller solar PV size. On the other hand, the size of BG, battery bank, and converter is not affected by the solar radiation rate. From

TABLE 6. The optimal architecture of the proposed system for average solar radiation.

BW (MHz)	PV (kW)		BG (kW)		Battery (units)		Converter (kW)	
	20W	40W	20W	40W	20W	40W	20W	40W
5	2.5	3.5	1	1	64	64	0.1	0.1
10	2.5	5	1	1	64	64	0.1	0.1
15	3.5	5.5	1	1	64	64	0.1	0.1
20	5	6	1	1	64	64	0.1	0.1

TABLE 7. Summary of technical criteria for the proposed system varying R ($kWh/m^2/day$) under 10MHz BW.

R	PV (kW)		BG (kW)		Battery (units)		Converter (kW)	
	20W	40W	20W	40W	20W	40W	20W	40W
4	2.5	4.5	1	1	64	64	0.1	0.1
4.5	2.5	4.5	1	1	64	64	0.1	0.1
5	2.5	4.5	1	1	64	64	0.1	0.1
5.5	2	4	1	1	64	64	0.1	0.1

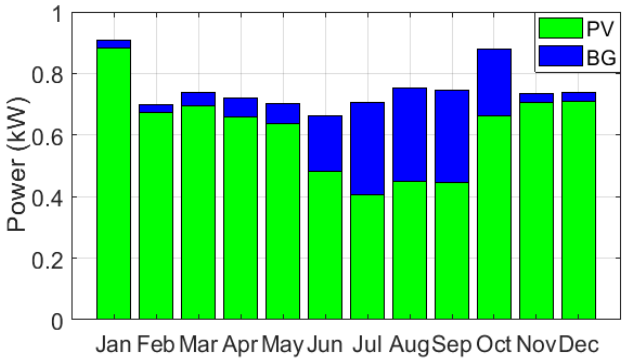

FIGURE 15. Monthly power contribution by hybrid PV/BG system for P_{TX} = 20W, and BW = 10MHz.

Table 6 and 7, it is observed that the size of the converter and battery bank remain constant for both P_{TX} = 20W and P_{TX} = 40W which enhance the system reliability. The size of the converter and the number of units of the battery can be calculated respectively by using (7) and (18). Additionally, in order to support the higher system BW and transmission power, a large number of solar PV panel is required.

The statistics of monthly output power by the RES for average solar radiation and biomass available under 10MHz bandwidth is shown in Fig. 15. Monthly power contribution curves imply that the maximum power generation occurred by the solar PV in most of the time, due to the increased sunshine hours and solar radiation. However, solar PV and biomass resources often complement each other. This complimentary effect is even greater during seasonal changes. In the case of night/dirty weather, biomass generator contributes higher power while in the case of the adequate intensity of sunlight, solar PV produces higher power. Additionally, backup power is provided by the battery bank, which was charged by the RES during the peak generation. So, the integration of BG and solar PV along with battery bank will ensure energy generation throughout the year.

The capacity of solar PV panel with respect to the bandwidth variation under different transmission power is presented in Fig. 16. Notably, the optimal size of the solar PV is rising linearly with the increment of system bandwidth

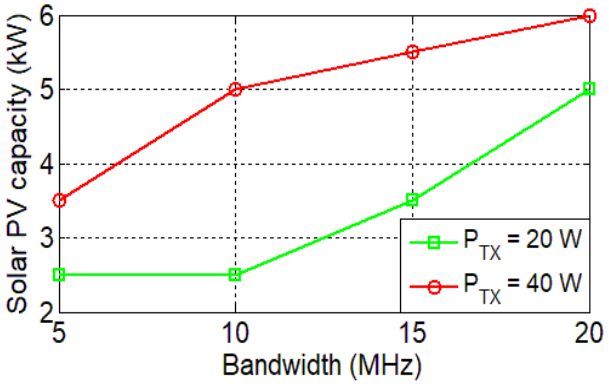

FIGURE 16. Solar PV array capacity vs. system bandwidth under different P_{TX}.

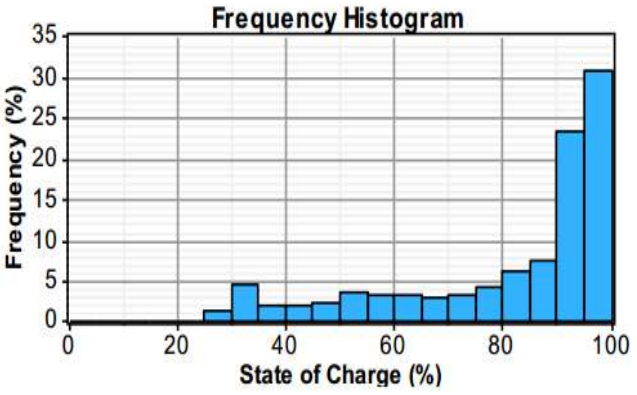

FIGURE 18. Annual frequency histogram of SOC for P_{TX} = 40W, BW = 10MHz, and R_{avg}.

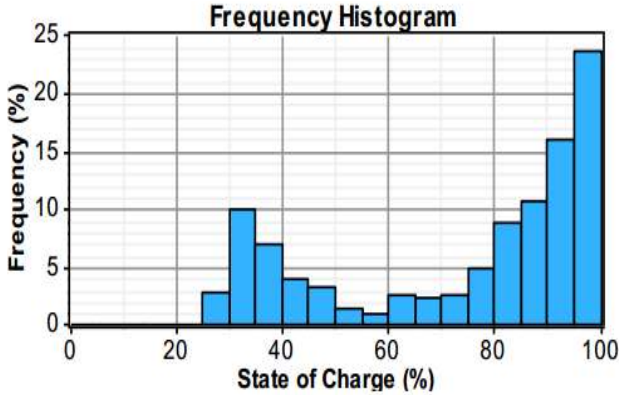

FIGURE 17. Annual frequency histogram of SOC for P_{TX} = 20W, BW = 10MHz, and R_{avg}.

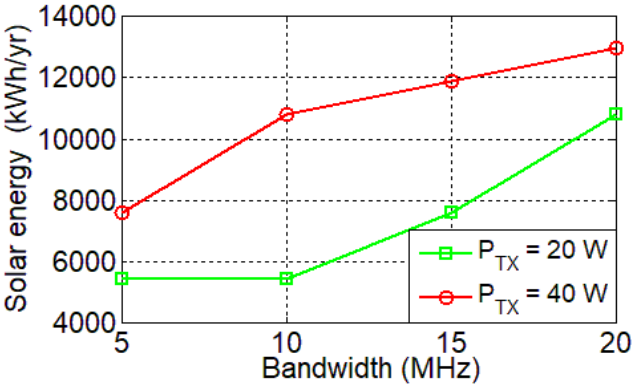

FIGURE 19. Solar PV energy vs. system bandwidth under different P_{TX}.

to cope with the higher energy demand of BS. It is also noticeable that P_{TX} = 40W curve is staying in an upper position which indicates that the higher transmission power required higher solar PV capacity than the lower one.

Fig. 17 and 18 demonstrate the annual frequency histogram of a battery bank respectively for macro BS of P_{TX} = 20W and P_{TX} = 40W. The frequency histogram of P_{TX} = 20W indicates that the battery bank is in a minimal SOC for approximately 2% of the year and high SOC for approximately 23% of the year. Thus, the battery bank replacement is essential during the project time.

2) ENERGY YIELD ANALYSIS

In this subsection, the annual energy generated by the solar PV panel (E_{PV}) and biomass generator (E_{BG}) along with excess electricity has been analyzed focusing on the optimal system criteria. The battery bank autonomy, throughput, lifetime, and biomass energy consumption have been thoroughly investigated for different network configurations. Moreover, energy sharing technique among the neighboring BSs has been incorporated for saving energy.

a: SOLAR PV PANEL

Table 6 and 7 summarize the optimal size of solar PV panel for different network configurations. As refer to Table 6, the capacity of the PV array is 5 kW for P_{TX} = 40W and BW = 10MHz. So, the Sharp ND-250QCs module is a proper selection. According to the (2), the solar PV array consists of 20 Sharp ND-250QCs modules (5kW/250W = 20). Five of these modules are connected in a series and four are in a parallel position. This placement of modules is to satisfy the requirements of the solar energy controller considered as an energy management unit in this paper.

The annual energy generated by the solar PV panel based on the average solar radiation for macrocell BS under 10MHz bandwidth can be calculated by using (1): $E_{PV} = 2.5\ kW \times 4.59 \times 0.9 \times 365\ days/year = 3,769.53\ kWh/yr$. Besides, a dual-axis tracking mode of solar PV panel increases the total amount of energy by 43.4% to be 5,405 kWh/yr. In a similar process, energy generated for all other configuration is calculated. The annual energy generated by the solar PV panel for different network configurations is presented in Fig. 19. All the curves are upward trending like Fig. 16, which implies that a higher system BW and P_{TX} clearly corresponded to higher annual energy contribution by the solar PV panel.

b: BIOMASS GENERATOR

Energy generated by the biomass generator can be determined by using (3) and (4) as follows: P_{BG} = 1.62 t/year (BM_{TA}) × 3,411.33 KCal/Kg (CV_{BM}) × 0.30 (η_{BG}) × 1000 / (365 × 860 × 10.67 (t_{op})) = 0.509 kW and E_{BG} =

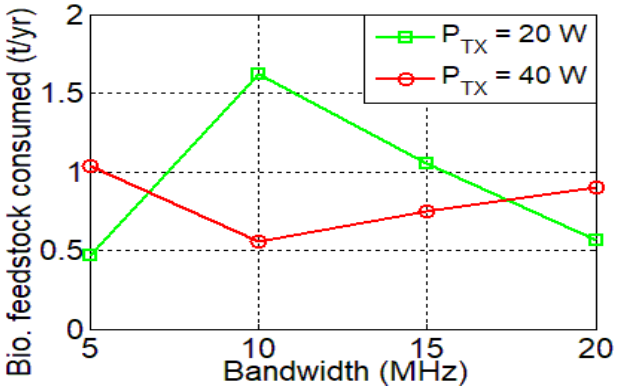

FIGURE 20. Bio. feedstock consumed with bandwidth for different P_{TX}.

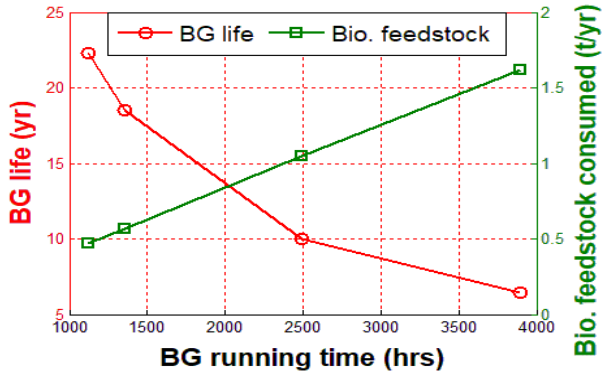

FIGURE 21. BG life and Bio. feedstock consumed with BG operating hour.

0.509 (P_{BG}) × 365 × 24 × 0.26 (capacity factor) = 1,161 kWh/yr for macro BS, under BW = 10MHz, and R_{avg} = 4.59 $kWh/m^2/day$ configuration. In an analogous process, energy generated for all configuration is calculated.

The amount of bio. feedstock consumption with the variation of system BW and BG running time are respectively shown in Fig. 20 and 21. Fig. 21 also represents the impact of BG running time on the BG lifecycle. As seen, bio- feedstock consumption is proportional to the BG operation hours and a higher value of BG running time points out the higher annual energy contribution by the biomass generator as a consequence of less energy supplied by the solar PV panel. However, lower BG running time increases the BG lifetime and improves the system performance by means of a substantial reduction of CO_2.

c: EXCESS ELECTRICITY

HOMER calculates the battery losses (B_{loss}) 398 kWh/yr and converter losses (C_{loss}) 90 kWh/yr, for macro P_{TX} = 20W BS, BW = 10MHz, and R_{avg} = 4.59 $kWh/m^2/day$. Annual excess electricity (E_{Excess}) of the system can be determined by using (30): 5,405 kWh (E_{PV}) + 1,161 kWh (E_{BG}) - 5,044 kWh (E_{BS}) - 398 kWh (B_{loss}) - 90 kWh (C_{loss}) = 1,034 kWh/yr. The annual excess electricity generation for all other network setups can be found in the same way. The annual excess electricity generation for various BW including the annual energy contribution by the RES and losses are

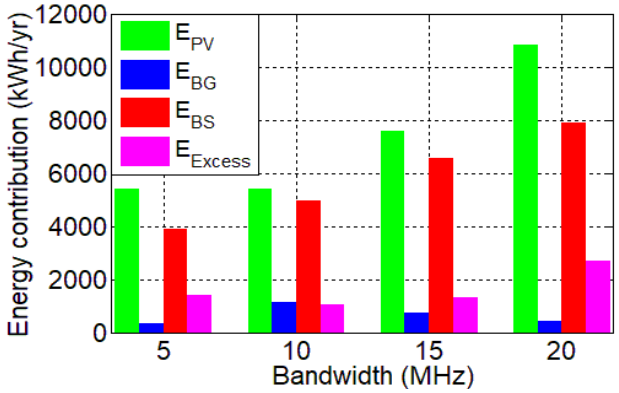

FIGURE 22. Annual energy breakdown for P_{TX} = 20W, and R_{avg}.

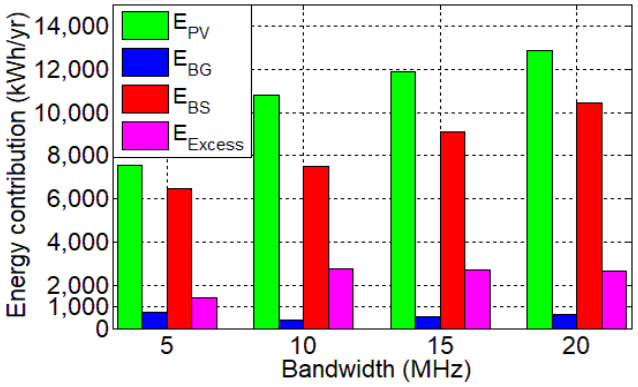

FIGURE 23. Annual energy breakdown for P_{TX} = 40W, and R_{avg}.

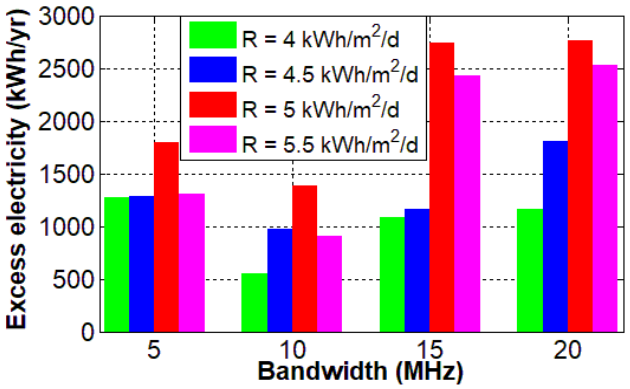

FIGURE 24. Excess electricity with BW for P_{TX} = 20W varying R_{avg}.

summarized in Fig. 22, 23, and 24. The greater value of E_{Excess} indicates the better system reliability as the mentioned scheme could independently meet the BS energy requirement without any support from external nonrenewable energy sources. Fig. 22 and 23 illustrate the annual excess electricity generation for the different system BW under average solar radiation. It is seen that the annual excess electricity is increases linearly with the increment of system BW for both P_{TX} = 20W and P_{TX} = 40W. It is happening because a higher value of system BW and P_{TX} represents the higher amount of energy demand. As a result, a higher amount of backup power and excess electricity are required. On the other

TABLE 8. Annual energy assessment for energy sharing mechanism.

BW (MHz)	E_{Excess} (kW) 20W	40W	I (Amp) 20W	40W	E_{loss} (kWh) 20W	40W	E_{share} (kWh) 20W	40W	E_{save} (%) 20W	40W
5	1386	1407	3.29	3.34	537	556.08	848.3	850.9	21.7	13.17
10	1034	2762	2.45	6.56	298.13	2137	735.8	625	14.85	8.35
15	1314	2724	3.12	6.47	485.05	2079	828.9	645	12.66	7.08
20	2687	2639	6.39	6.27	2028	1952.6	658.9	686.3	8.37	6.57

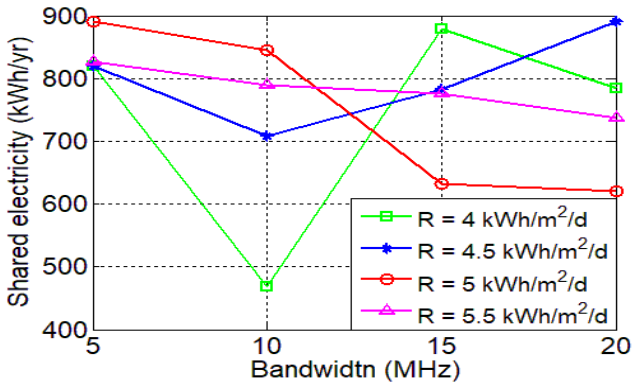

FIGURE 25. Shared electricity among neighboring BS for $P_{TX} = 20$W, and BW = 10MHz.

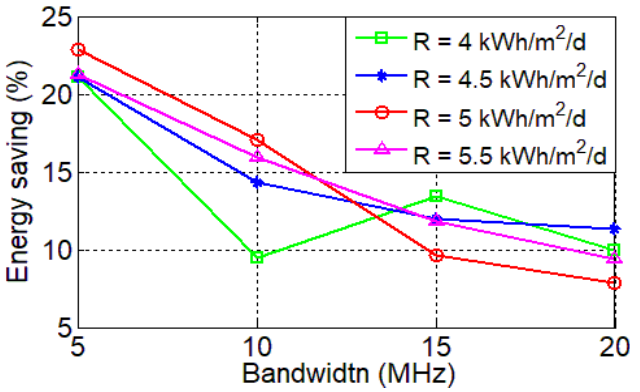

FIGURE 26. Energy-saving via energy cooperation mechanism for $P_{TX} = 20$W.

hand, Fig. 24 depicts that the excess electricity is proportional to the solar radiation rates since the sunlight intensity has a direct impact on solar PV panel capacity and solar energy generation as well.

d: ENERGY SAVING BY SHARING MODEL

Under the suggested network, the BSs would exchange energy among themselves in the possible shortest path to reduce the I^2R loss occurred in the conductor after fulfilling its own demand. In this model, we consider a transmission line whose resistance is 3.276 Ω per kilometer length that is found from the American Wire Gauge (AWG) standard conductor size table. The inter-site distance (ISD) is calculated as $\sqrt{3}$ times of cell radius (i.e. $\sqrt{3}R$) and the cell radius is 1000 m with 43 dBm transmit power. The total resistance of the transmission line between the two BSs is 5.67 Ω.

The green energy sharing model enhances network sustainability by forming a collaboration between the neighboring BSs. For remote sites, where the grid connection is not available, the energy sharing technique assists the BSs for the harvesting energy from locally available energy sources by maximum utilization of RES through subsequent energy and cost-saving. Fig. 25 shows the amount of shared energy for 10MHz macro BS which is calculated using (33). The percentage of energy-saving by applying the energy sharing technique is determined by (34) and presented in Fig. 26. Fig. 25 and 26 depict that the amount of shared energy and percentage of energy-saving for macro BS is respectively 10 kWh and 4%. Table 8 summarizes the sharable energy, energy losses, and percentage of energy-saving for diverse BW considering the average solar intensity.

TABLE 9. Annual energy sharing for various resistance loss under $P_{TX} = 20$W, and BW = 10MHz.

Resistance (%)	Resistance (Ω)	E_{loss} (kWh)	E_{share} (kWh)	E_{save} (%)
100	5.670	298.13	735.88	0 (reference)
95	5.386	283.2	750.8	2.03
90	5.103	268.3	765.7	4.06
85	4.819	253.4	780.6	6.08
80	4.536	238.5	795.5	8.11

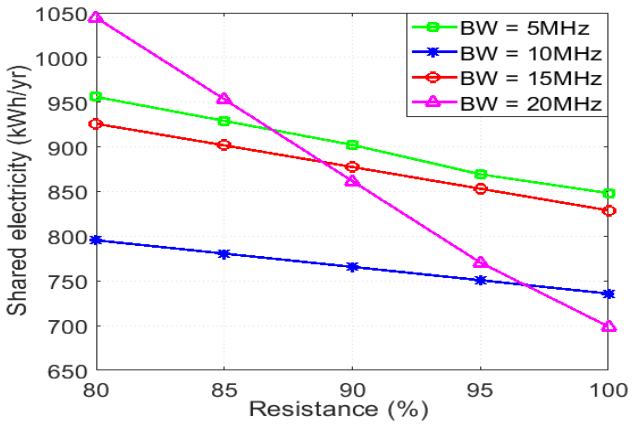

FIGURE 27. Shared electricity under different resistance for $P_{TX} = 20$W.

Fig. 27 and Table 9 illustrate the amount of transferred energy between the neighboring BSs with the variation of resistance of the power line. In line with our expectation, all the curves follow the analogous shape to reach their minimum values, which implies that a lower value of line resistance offers smaller line losses and incurs a higher amount of energy sharing. Table 9 also expresses that 5% less resistance will save up to 5% energy and thus improves energy sharing up to 2.03%.

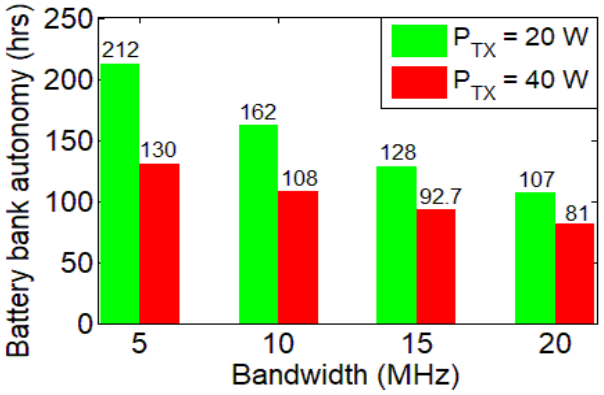

FIGURE 28. Variation of battery bank autonomy with bandwidth for different P_{TX}.

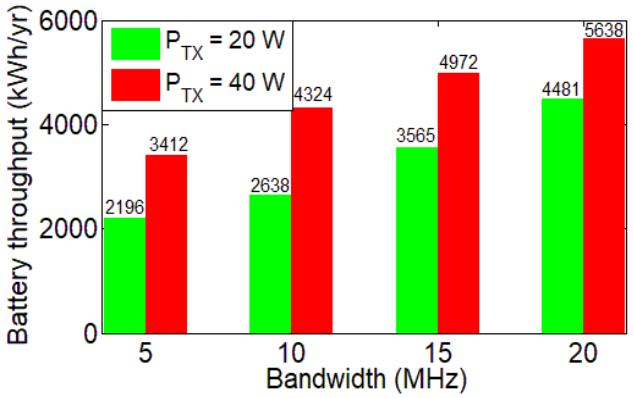

FIGURE 29. Variation of battery bank throughput with bandwidth for different P_{TX}.

e: BATTERY BANK

The total number of battery units that are required for both $P_{TX} = 20$W and $P_{TX} = 40$W of the proposed configuration is 64; connected 8 in series and 8 in parallel. The battery bank can support the macro BS load autonomously for 162 hours, which is determined using (16) under $P_{TX} = 20$W, BW = 10MHz, and R_{avg} configuration: ($N_{batt} = 64 \times V_{nom} = 6\ V \times Q_{nom} = 360\ Ah \times B_{DOD} = 0.7 \times 24\ h$)/daily load, $L_{BS} = 14.336$ kWh. In a similar way, the battery bank autonomy for all network configuration can be determined. Fig. 28 exhibits the battery bank annual autonomy (B_{aut}) for average solar radiation and battery bank throughput (Q_{tp}) for various system BW which is presented in Fig. 29. According to Fig. 28, B_{aut} gradually decreases with respect to the system bandwidth as the daily BS energy requirement (L_{BS}) increases correspondingly. It is noteworthy that the battery bank throughput is mostly affected by the BS energy demand and BW variation. As a result, a higher value of system bandwidth and transmission power increases the BS energy demand. As refer to (16), a higher value of L_{BS} uplifts the battery bank throughput.

A higher value of B_{aut} and B_{life} are preferable for reliable and cost-effective green mobile network to carry the BS load for a long time. Better performance of B_{life} inherently minimizes the replacement cost in terms of overall NPC.

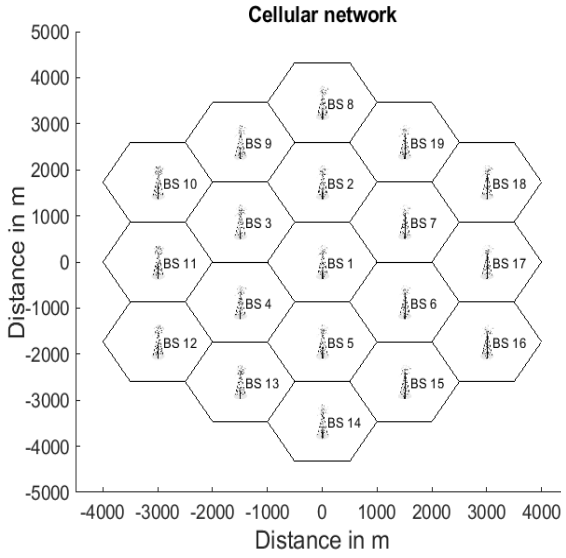

FIGURE 30. Two-tier hexagonal cellular system with 19 BS.

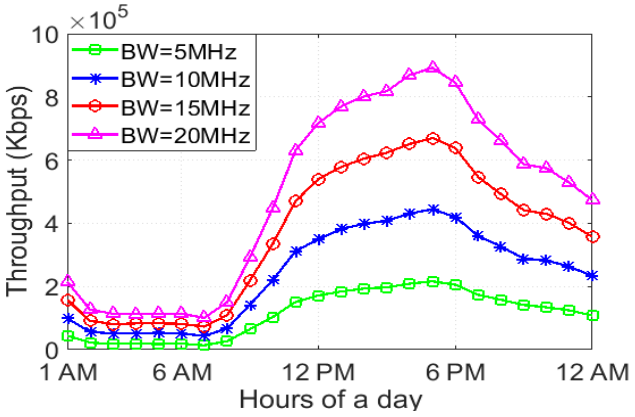

FIGURE 31. Throughput performance over a day for different system bandwidth.

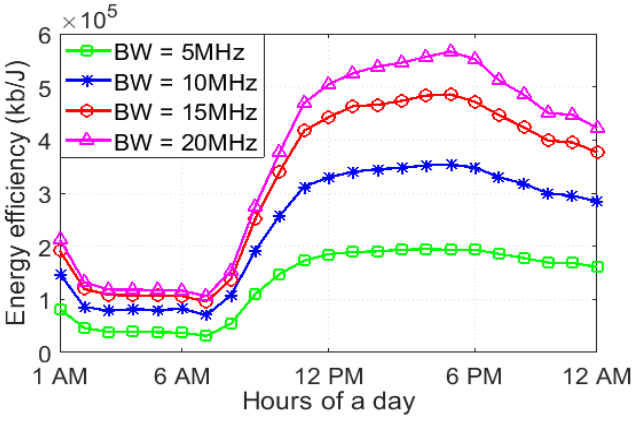

FIGURE 32. Energy efficiency vs. BW for a single day.

3) ENERGY EFFICIENCY ANALYSIS

In this work, a two-tier LTE cellular network with 19 base stations along with hexagonal shape has been considered as shown in Fig. 30, where one BS is placed at the center of hexagonal and the other eighteen BSs are put around the

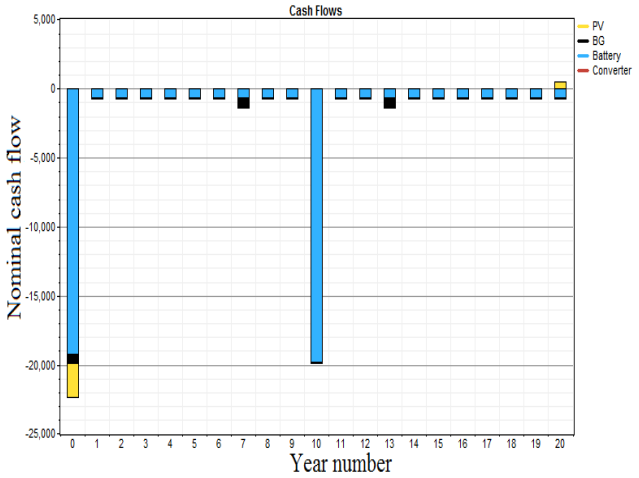

FIGURE 33. Cash flow summary of the proposed system for BW = 10MHz, and P_{TX} = 20W.

TABLE 10. Cost breakdown for macro BS under average solar radiation, and P_{TX} = 20W.

BW (MHz)	CC ($)	RC ($)	OMC ($)	FC ($)	SV ($)	NPC ($)
5	22400	10006	7316	152	-161	39713
10	22400	10909	7195	525	-304	40725
15	23400	10349	7572	339	-197	41463
20	24900	10204	7611	184	-442	42457

TABLE 11. Cost breakdown for macro BS under BW = 10MHz, and P_{TX} = 40W.

R ($kWh/m^2/day$)	CC ($)	RC ($)	OMC ($)	FC ($)	SV ($)	NPC ($)
4	21680	11881	7949	933	-170	43273
4.5	24400	10347	7678	336	-255	42507
5	24400	10006	7545	168	-253	41866
5.5	23900	10188	7494	172	-400	41353

hexagonal to identify the interference. It is also considered that the network is randomly distributed over time and space according to the dynamic load profile of Fig. 9. The BSs are mainly supplied by the hybrid PV/BG scheme and the backup power is provided by the storage device as well as the energy sharing mechanism. The throughput performance of one day for various system BW is presented in Fig. 31. It is obvious that a higher system BW offers a better throughput performance and the throughput curves are in the similar manner to the traffic pattern of Fig. 9. This happened because the traffic density is directly related to the number of resource blocks and RBs related to the throughput. Additionally, the throughput gap is very cabalistic during higher traffic density. On the other hand, a comparison of energy efficiency for different BW is illustrated in Fig. 32. The term 'energy efficiency' is defined as the ratio of total network throughput to total power consumed by the network. The upper value of EE is always preferable, which has a positive impact on network power consumption. As a consequence, higher energy efficiency is obtained for higher throughputs.

4) COST ANALYSIS

Tables 10, 11,and 12 summarize different types of costs associated with the hybrid solar PV/BG powered cellular base

TABLE 12. Cost breakdown for macro BS under BW = 10MHz, and P_{TX} = 40W.

Components	CC	RC	OMC	FC	SV	NPC
PV	5000	0	540	0	-271	5269
BG	660	194	144	181	-166	1014
Battery	19200	9991	6914	0	0	36105
Converter	40	15	11	0	-7	59
Total cost	**24900**	**10201**	**7609**	**181**	**-444**	**42447**

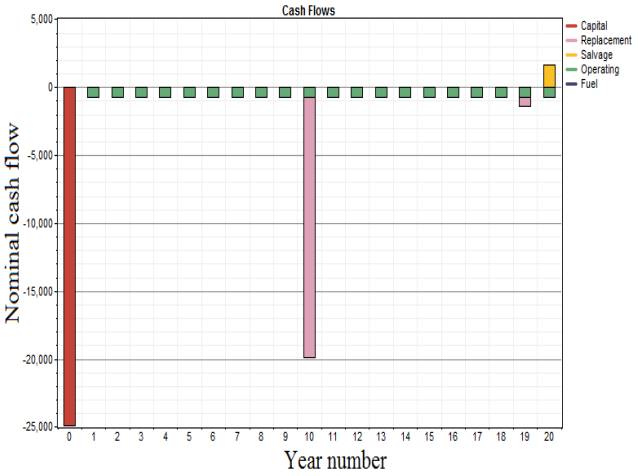

FIGURE 34. Cash flow summary of the proposed system for BW = 10MHz, and P_{TX} = 40W.

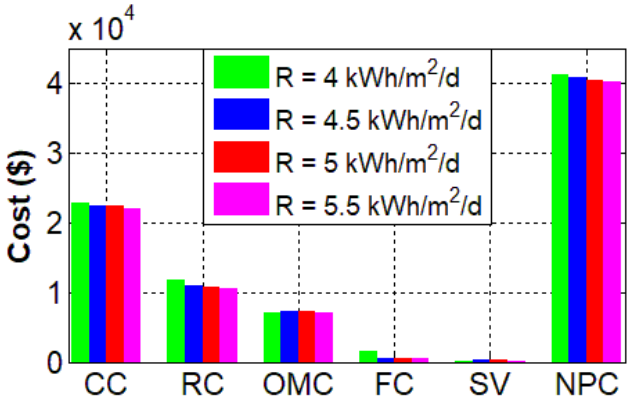

FIGURE 35. Comparison of cost analysis varying radiation for BW = 10MHz, and P_{TX} = 20W.

stations. From the numerical results, it is seen that the initial capital cost has the maximum value among the different types of expenses. Besides, Table 12 indicates that energy generation from the RES involves a significant amount of replacement cost due to the smaller lifecycle of the battery bank. On the other hand, the negative salvage value of solar PV, BG, and converter means that these components will offer cashback at the end of the project. Based on the cost breakdown, the nominal cash flow summary for P_{TX} = 20W and P_{TX} = 40W are respectively shown in Fig. 33 and 34 under the average value of solar/biomass availability.

The cost breakdown for the initial capital cost (CC), replacement cost (RC), operation and maintenance cost (OMC), salvage value (SV), and net present cost (NPC) that occurred during the project lifetime are shown in this

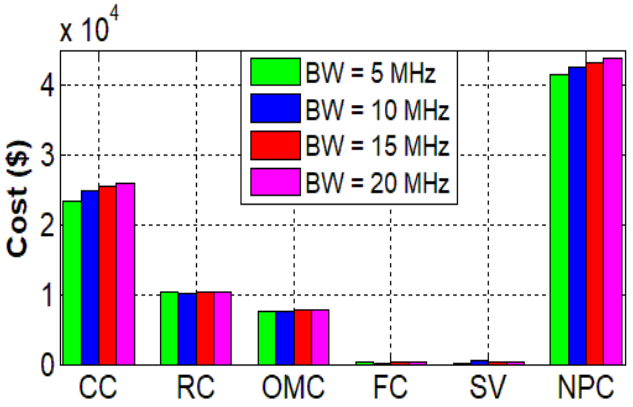

FIGURE 36. Comparison of cost analysis varying radiation for BW = 10MHz, and P_{TX} = 40W.

subsection. The CC is paid once at the starting of the project, which is related to the size of the system. According to the Table 12, the fixed CC under 10MHz bandwidth is $24,900. The breakdown of the CC is as follows: (i) for solar PV (size 5 kW × cost $1,000/1kW = $5,000); (ii) for BG (size 1 kW × cost $660/1kW = $660); (iii) for battery (64 units × cost $300/unit = $19,2000); and (iv) for converter (size 0.1 kW × cost $400/1kW = $40).

There is a bulk amount of replacement cost ($10,201) because the lifetime of the battery, BG, and converter are smaller than the project lifetime. On the other hand, the lifetime of the solar PV panel is 25 years, which is larger than the project lifetime. The total OMC cost of the hybrid power system under P_{TX} = 40W is $7,609 and the annual OMC cost of the project is $704. The number of battery units and per unit battery cost are the key factors of increasing CC and OMC of the system.

The remaining cost of each component at the end of the project duration is known as salvage value. Solar PV panel has the highest SV of $271, which is calculated by using (44). The salvage value of BG and converter is $166, and $7 respectively, thus the total salvage value of the project is $444. The total NPC involves all types of costs that occur during the project lifetime and determined in each year of the project as follows: Capital cost $24,900+ Replacement cost $10,201+ OMC $7,609+ Fuel cost $181-Salvage value $444, which equals $42,447.

The above cost assessment has been done considering the nominal system architecture. Different types of costs associated with the macro BS considering the average daily solar radiation (4.59 kWh/m^2) and average biomass available (9 t/day) are respectively provided in Fig. 35 and 36. All the figures demonstrate that higher system BW pushes up the associated costs, and the higher solar intensity pulls down the cost. It is also obvious that CC of the components is the highest cost and RC is the second-highest due to the replacement of the battery bank.

An explicit comparison of the NPC with the increment of system BW and biomass price is respectively demonstrated in Fig. 37 and 38. All the NPC curves are decreasing in

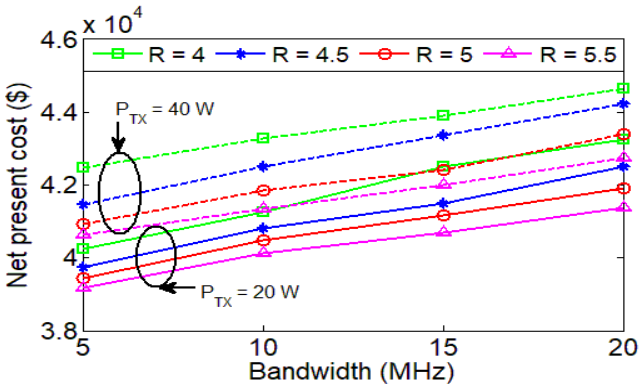

FIGURE 37. NPC comparison varying solar radiation.

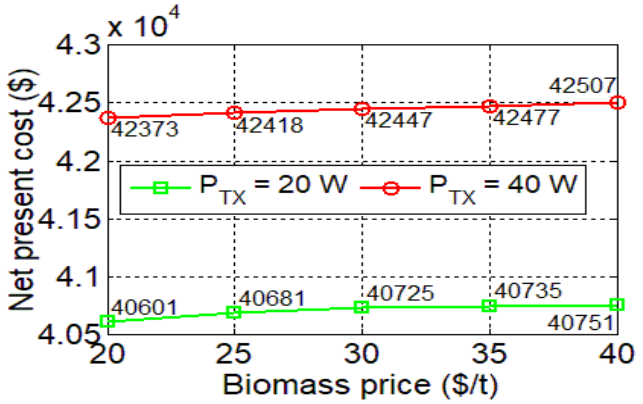

FIGURE 38. NPC vs. biomass price for BW = 10MHz.

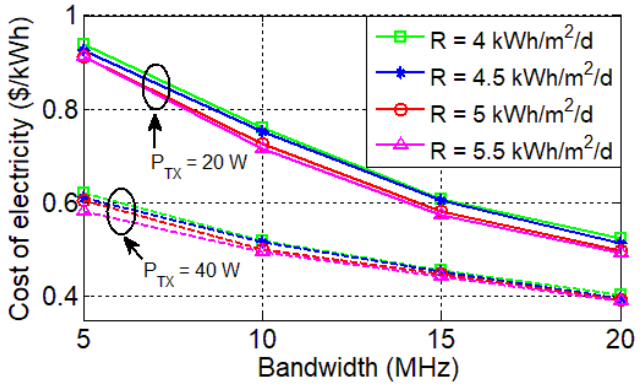

FIGURE 39. COE comparison varying solar radiation.

nature to reach the bottom line with respect to the increment of system BW and solar intensity. According to equation (22) to (26), the higher system BW upholds the base station power consumption. In order to support the higher energy demand, a higher value of solar PV panel and BG capacity is required which subsequently increases the total net present cost (NPC). However, the higher transmission power and biomass power are also responsible for the increment of NPC.

The impact of variation of solar intensity and system BW on the cost of electricity is demonstrated in Fig. 39. The COE curves are diminishing dramatically with the increment of system BW and solar radiation rate. Moreover, the lower transmission power requirement introduces higher COE than

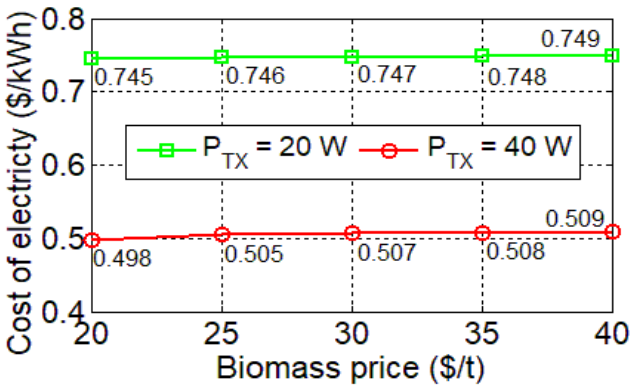

FIGURE 40. COE vs. biomass price for BW = 10MHz.

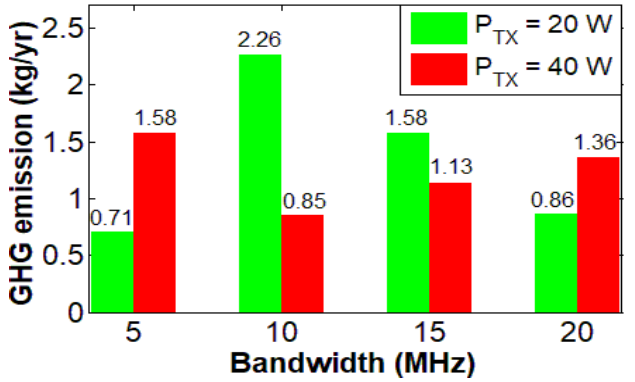

FIGURE 41. GHG emissions vs. system bandwidth for average solar radiation.

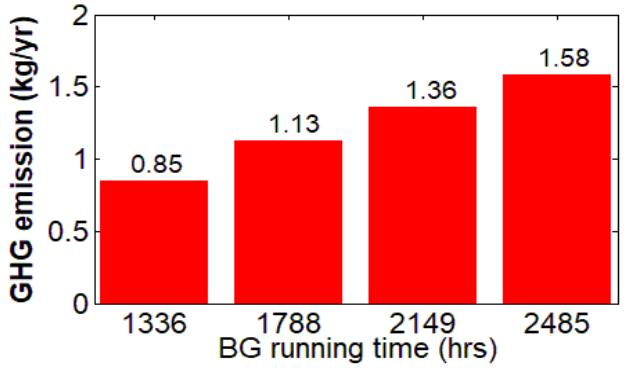

FIGURE 42. GHG emissions vs. BG running time for average solar radiation.

the higher transmission power. So, the negative slope of the electricity curve implies that a better COE can be obtained by operating the BS at higher system BW and higher transmission power. For higher BW and P_{TX}, the hybrid system generates a higher amount of energy and thus decreases the corresponding capital cost. As a result, the higher system BW offers lower COE. Finally, the COE curves under different transmission power can be explored by varying the biomass price as shown in Fig. 40. As a matter of fact, lower transmission power and higher biomass price are accountable for the poor value of electricity generation cost.

TABLE 13. Pollutants for $P_{TX} = 20W$, and BW = 10MHz.

Pollutants	Emissions (Kg/yr)	
	20W	40W
Carbon dioxide	2.36	0.0815
Carbon monoxide	0.0105	0.00364
Unburned hydrocarbons	0.00117	0.000403
Particulate matter	0.000794	0.000274
Nitrogen oxides	0.094	0.0325

TABLE 14. The optimal size of the stand-alone solar PV scheme.

BW (MHz)	PV (kW)		Battery (units)		Converter (kW)	
	20W	40W	20W	40W	20W	40W
5	2.5	4	64	64	0.1	0.1
10	3.5	5	64	64	0.1	0.1
15	4.5	6	64	64	0.1	0.1
20	5	7	64	64	0.1	0.1

TABLE 15. The optimal size of the hybrid PV/DG scheme.

BW (MHz)	PV (kW)		DG (kW)		Battery (units)		Converter (kW)	
	20W	40W	20W	40W	20W	40W	20W	40W
5	3	5	1	1	64	64	0.1	0.1
10	4	6	1	1	64	64	0.1	0.1
15	5	6.5	1	1	64	64	0.2	0.1
20	5.5	8	1	1	64	64	0.2	0.1

5) GHG EMISSIONS

Due to the technological advancement, the higher volume carbon footprint of RES (especially biomass) can be maintained at a lower value. The premier carbon contents emanated by the proposed system for 10MHz bandwidth are counted in Table 13. Among the different pollutants, CO_2 is the main contributor to the GHG emission. Fig. 41 counts the pollution rate as well as annual GHG emissions for different network settings. In a hybrid solar PV/BG system, solar as an ideal energy source produces zero carbon contents where all of the GHG is emitted by the biomass generator only. The hybrid solar PV/BG system emits the highest amount of greenhouse gas for 10MHz and 15MHz bandwidth because of higher energy contribution by the biomass generator as seen from Fig. 22. Additionally, the impact of toxic-intensive GHG generated by the biomass generator is expressed in Fig. 42, which implies that a higher BG operating time promotes the carbon footprints, although there is a significant betterment in reliability and QoS. In general, solar radiation rate and solar cell size have a conducive effect on pollution minimization with upgrading the energy generated by the solar PV panel.

C. FEASIBILITY COMPARISON

In this subsection, the outcomes of the proposed system are compared with the stand-alone solar PV and hybrid PV/DG scheme keeping in mind the technical criteria namely, economic analysis, energy yield analysis and greenhouse gas emissions for ensuring the network sustainability.

An optimum size of individual components of the stand-alone solar PV and hybrid PV/DG system for the same network setting are respectively summarized in Table 14 and 15. As shown in tables, a large number of solar PV panels are required in order to satisfy the BS energy demand for both

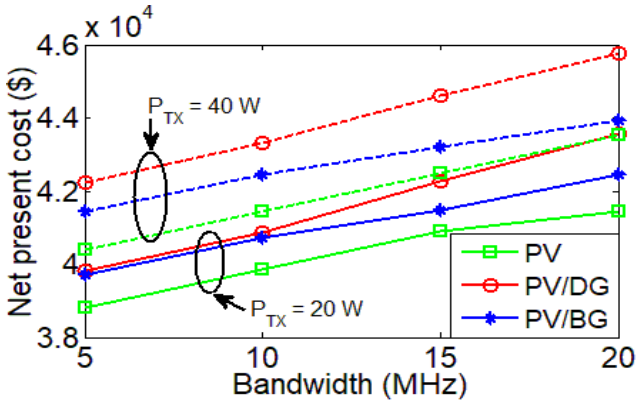

FIGURE 43. Comparison of NPC among different power supply scheme for R_{avg}.

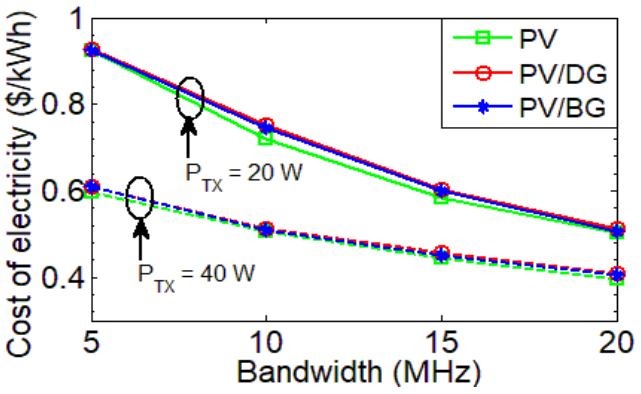

FIGURE 44. Comparison of COE among different power supply scheme for R_{avg}.

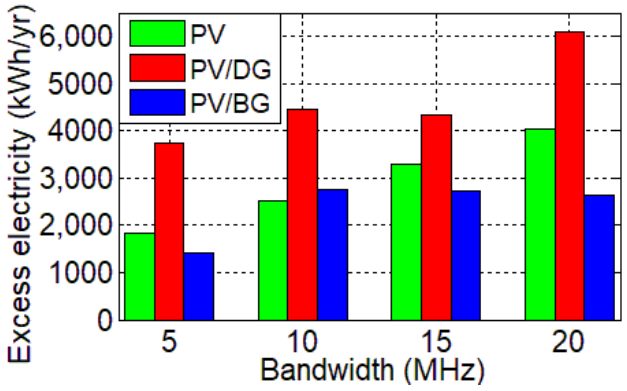

FIGURE 45. Comparison of excess electricity among different power supply scheme for $P_{TX} = 40$W and R_{avg}.

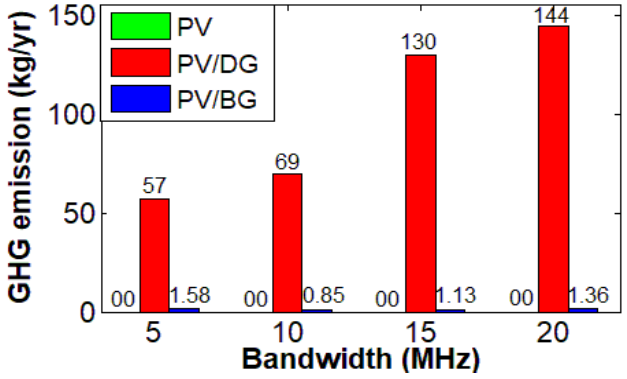

FIGURE 46. Comparison of GHG among different power supply scheme for $P_{TX} = 40$W, and R_{avg}.

TABLE 16. Emissions by different sources [25].

Fuels	Emissions (Kg/Kg fuel)
Rice Husk	1.49
Bituminous Coal	2.46
Natural Gas	1.93

solar PV and hybrid PV/DG powered systems which lead to a remarkable increase in NPC and COE. The hybrid solar PV/DG system has a higher solar PV capacity than the stand-alone solar PV system for making the system more reliable. Fig. 43 and 44 respectively compare the NPC and COE for the different types of supply systems assuming average solar intensity and available biomass. In line with our expectation, the hybrid PV/DG system has the highest NPC and COE because of the high fuel cost. On the other hand, the stand-alone solar PV system is less expensive. The proposed PV/BG system has a lower NPC and COE in comparison with the hybrid PV/DG system. Additionally, the hybrid PV/BG system provides greater reliability compared to using a stand-alone solar PV system because a single energy technology source solar energy generation may be outage depending on the weather condition. For a better understanding of the term 'reliability', an explicit comparison of excess electricity among the aforementioned supply systems is exhibited in Fig. 45. The hybrid solar PV/DG system has higher excess electricity than the stand-alone solar PV system for making the system more reliable.

In the end, a detailed comparison of GHG emission among different supply systems is demonstrated in Fig. 46 for R_{avg} and $P_{TX} = 40$W. As an ideal renewable energy source, the stand-alone solar PV system produces zero GHG emissions. On the other hand, BS demand is fulfilled by the huge amount of fuel burning in a hybrid PV/DG powered system, which involves higher operational expenditure and carbon contents.

Despite the very small amount of GHG emissions, hybrid solar PV/BG system is superior to the stand-alone solar PV and hybrid solar PV/DG system because of the following reasons: (i) PV/BG system provides greater sustainability due to the complementary effect of solar PV and BG; and (ii) PV/BG system indirectly minimizes CO_2 emission by reducing the biomass burning in cooking purpose. In other words, biomass burning has a hostile impact on the environment which is shown in Table 16 [25]. However, the proposed hybrid solar PV/BG system can save a significant amount of GHG emissions as compared to the hybrid solar PV/DG.

VI. CONCLUSION

This study examined the feasibility and effectiveness of the integration of a solar PV system with the biomass resource generator for powering the off-grid macro BSs in Bangladesh to minimize the NPC and GHG emissions. Green energy

sharing mechanism has also been incorporated for enhancing the energy efficiency by maximum utilization of RES. For ensuring long term sustainability and reliability, the performance of the renewable energy-based system along with sufficient energy storage devices has been analyzed in terms of three key aspects: (i) energy yield analysis, (ii) economic analysis, and (iii) GHG emission. Extensive simulation has been carried out over the entire project time using the HOMER software in order to determine the optimal system architecture, energy-saving, capital cost and carbon footprint considering the effect of solar radiation, and bandwidth variation. The simulation results reveal that the proposed system is more eco-friendly and technically feasible. It can also satisfy the BS energy demand independently without support from the battery bank. However, the energy storage device can feed the BS load autonomously for 162 hours (P_{TX} = 20W) and 108 hours (P_{TX} = 40W) without any external sources during the deficiency of solar or biomass energy, which is a sufficient time to fix the hybrid system. The performance of the network is also evaluated in terms of throughput and energy efficiency metrics. In summary, energy sharing technique can save a considerable amount of energy and capital cost by improving energy efficiency. For P_{TX} = 20W, and BW = 10MHz total energy generated from the hybrid system is 6,566 kWh (82% from solar PV and 18% from BG) and provides excess electricity of 1,034 kWh, which indicates the increased level of reliability ensuring zero outage. Additionally, the performance of the proposed system has been compared with the stand-alone solar PV and hybrid PV/DG system in terms of the performance parameters. The numerical outcomes demonstrate that the proposed system has the potential to save up to $797 (representing 1.84%) of the NPC and decrease GHG emissions to 98% over a hybrid PV/DG system (under P_{TX} = 40W and BW = 10MHz). Thus, the renewable energy powered off-grid BSs will be a cost-effective, reliable and sustainable solution assuring clean energy for the cellular network operators.

REFERENCES

[1] Ericsson. *Mobile Subscriptions Q1 2019*. Accessed: Sep. 20, 2019. [Online]. Available: https://www.ericsson.com/en/mobility-report/reports/june-2019/mobile-subscriptions-q1-2019

[2] GSMA. *Country Overview: Bangladesh*. Accessed: Sep. 20, 2019. [Online]. Available: https://www.gsmaintelligence.com/research/?file=a163eddca009553979bcdfb8fd5f2ef0&download

[3] GSMA, London, U.K. (Jan. 2010). *Community Power: Using Mobile to Extend the Grid*. Accessed: Sep. 20, 2019. [Online]. Available: https://www.gsma.com/mobilefordevelopment/wp-content/uploads/2012/05/Community-Power-Using-Mobile-to-Extend-the-Grid-January-2010.pdf

[4] J. Wu, Y. Zhang, M. Zukerman, and E. K.-N. Yung, "Energy-efficient base-stations sleep-mode techniques in green cellular networks: A survey," *IEEE Commun. Surveys Tuts.*, vol. 17, no. 2, pp. 803–826, 2nd Quart., 2015.

[5] A. Jahid and M. S. Hossain, "Energy-cost aware hybrid power system for off-grid base stations under green cellular networks," in *Proc. 3rd Int. Conf. Electr. Inf. Commun. Technol. (EICT)*, Khulna, Bangladesh, Dec. 2017, pp. 1–6.

[6] A. Jahid and S. Hossain, "Dimensioning of zero grid electricity cellular networking with solar powered off-grid BS," in *Proc. 2nd Int. Conf. Electr. Electron. Eng. (ICEEE)*, Rajshahi, Bangladesh, Dec. 2017, pp. 1–4.

[7] A. Aris and B. Shabani, "Sustainable power supply solutions for off-grid base stations," *Energies*, vol. 8, no. 10, pp. 10904–10941, Sep. 2015.

[8] GSMA. *Extending the Grid: Bangladesh Market Analysis*. Accessed: Sep. 10, 2019. [Online]. Available: http://www.gsma.com/mobilefordevelopment/wp-content/uploads/2013/03/GPM-Market-Analysis-Bangladesh.pdf

[9] *World Energy Outlook 2018*. Accessed: Sep. 20, 2019. [Online]. Available: https://www.iea.org/weo2018/

[10] A. Jahid, A. B. Shams, and M. F. Hossain, "Dynamic point selection CoMP enabled hybrid powered green cellular networks," *Comput. Electr. Eng.*, vol. 72, pp. 1006–1020, Nov. 2018.

[11] M. H. Alsharif, R. Nordin, and M. Ismail, "Energy optimisation of hybrid off-grid system for remote telecommunication base station deployment in malaysia," *EURASIP J. Wireless Commun. Netw.*, vol. 2015, no. 1, pp. 1–16, Dec. 2015.

[12] P. Gandotra, R. K. Jha, and S. Jain, "Green communication in next generation cellular networks: A survey," *IEEE Access*, vol. 5, pp. 11727–11758, 2017.

[13] V. Chamola and B. Sikdar, "Solar powered cellular base stations: Current scenario, issues and proposed solutions," *IEEE Commun. Mag.*, vol. 54, no. 5, pp. 108–114, May 2016.

[14] A. Jahid, M. S. Islam, M. S. Hossain, M. E. Hossain, M. K. H. Monju, and M. F. Hossain, "Toward energy efficiency aware renewable energy management in green cellular networks with joint coordination," *IEEE Access*, vol. 7, pp. 75782–75797, 2019.

[15] H. Ghazzai, E. Yaacoub, A. Kadri, H. Yanikomeroglu, and M.-S. Alouini, "Next-generation environment-aware cellular networks: Modern green techniques and implementation challenges," *IEEE Access*, vol. 4, pp. 5010–5029, 2016.

[16] A. Jahid and M. S. Hossain, "Feasibility analysis of solar powered base stations for sustainable heterogeneous networks," in *Proc. IEEE Region Humanitarian Technol. Conf. (R-HTC)*, Dhaka, Bangladesh, Dec. 2017, pp. 686–690.

[17] M. S. Hossain, B. Kumar Raha, D. Paul, and E. Haque, "Optimization and generation of electrical energy using wind flow in rural area of bangladesh," *Res. J. Appl. Sci., Eng. Technol.*, vol. 10, no. 8, pp. 895–902, Jul. 2015.

[18] R. T. Jacob and R. Liyanapathirana, "Technical feasibility in reaching renewable energy targets; case study on australia," in *Proc. 4th Int. Conf. Electr. Energy Syst. (ICEES)*, Chennai, India, Feb. 2018, pp. 630–634.

[19] S. Cordiner, V. Mulone, A. Giordani, M. Savino, G. Tomarchio, T. Malkow, G. Tsotridis, A. Pilenga, M. L. Karlsen, and J. Jensen, "Fuel cell based hybrid renewable energy systems for off-grid telecom stations: Data analysis from on field demonstration tests," *Appl. Energy*, vol. 192, pp. 508–518, Apr. 2017.

[20] A. Chauhan and R. P. Saini, "A review on integrated renewable energy system based power generation for stand-alone applications: Configurations, storage options, sizing methodologies and control," *Renew. Sustain. Energy Rev.*, vol. 38, pp. 99–120, Oct. 2014.

[21] NASA. *Surface Meteorology and Solar Energy: A Renewable Energy Resource*. Accessed: Sep. 10, 2019. [Online]. Available: https://eosweb.larc.nasa.gov/sse/

[22] M. A. H. Mondal and A. K. M. S. Islam, "Potential and viability of grid-connected solar PV system in bangladesh," *Renew. Energy*, vol. 36, no. 6, pp. 1869–1874, Jun. 2011.

[23] M. S. Hossain, A. Jahid, and M. F. Rahman, "Dynamic load management framework for off-grid base stations with hybrid power supply," in *Proc. 4th Int. Conf. Electr. Eng. Inf. Commun. Technol. (iCEEiCT)*, Dhaka, Bangladesh, Sep. 2018, pp. 336–341.

[24] Huawei. *Mobile Networks Go Green*. Accessed: Sep. 10, 2019. [Online]. Available: http://www.huawei.com/en/abouthuawei/publications/communicaite/hw-082734.htm

[25] P. K. Halder, N. Paul, and M. R. A. Beg, "Assessment of biomass energy resources and related technologies practice in bangladesh," *Renew. Sustain. Energy Rev.*, vol. 39, pp. 444–460, Nov. 2014.

[26] A. K Hossain and O. Badr, "Prospects of renewable energy utilisation for electricity generation in bangladesh," *Renew. Sustain. Energy Rev.*, vol. 11, no. 8, pp. 1617–1649, Oct. 2007.

[27] M. S. Islam, R. Akhter, and M. A. Rahman, "A thorough investigation on hybrid application of biomass gasifier and PV resources to meet energy needs for a northern rural off-grid region of Bangladesh: A potential solution to replicate in rural off-grid areas or not?" *Energy*, vol. 145, pp. 338–355, Feb. 2018.

[28] Food and Agriculture Organization. (Apr. 2018). *Rice Market Monitor*. Accessed: Sep. 10, 2019. [Online]. Available: http://www.fao.org/3/I9243EN/i9243en.pdf
[29] A. S. N. Huda, S. Mekhilef, and A. Ahsan, "Biomass energy in bangladesh: Current status and prospects," *Renew. Sustain. Energy Rev.*, vol. 30, pp. 504–517, Feb. 2014.
[30] M. Ahiduzzaman and A. S. Islam, "Energy utilization and environmental aspects of rice processing industries in bangladesh," *Energies*, vol. 2, no. 1, pp. 134–149, Mar. 2009.
[31] A. Jahid, A. S. Ahmad, and M. F. Hossain, "Energy efficient BS cooperation in DPS CoMP based cellular networks with hybrid power supply," in *Proc. 19th Int. Conf. Comput. Inf. Technol. (ICCIT)*, Dhaka, Bangladesh, Dec. 2016, pp. 93–98.
[32] A. Jahid, A. B. Shams, and M. F. Hossain, "Energy efficiency of JT CoMP based green powered LTE—A cellular networks," in *Proc. Int. Conf. Wireless Commun., Signal Process. Netw. (WiSPNET)*, Chennai, India, Mar. 2017, pp. 1739–1745.
[33] K. Kanwal, G. A. Safdar, M. Ur-Rehman, and X. Yang, "Energy management in LTE networks," *IEEE Access*, vol. 5, pp. 4264–4284, 2018.
[34] S. Hossain, A. Jahid, and F. Rahman, "Quantifying potential of hybrid PV/WT power supplies for off-grid LTE base station," in *Proc. Int. Conf. Comput., Commun., Chem., Mater. Electron. Eng. (IC4ME2)*, Rajshahi, Bangladesh, Feb. 2018, pp. 1–5.
[35] B. Xu, Y. Chen, J. Requena Carrion, J. Loo, and A. Vinel, "Energy-aware power control in energy cooperation aided millimeter wave cellular networks with renewable energy resources," *IEEE Access*, vol. 5, pp. 432–442, 2017.
[36] A. Jahid and S. Hossain, "Intelligent energy cooperation framework for green cellular base stations," in *Proc. Int. Conf. Comput., Commun., Chem., Mater. Electron. Eng. (ICME)*, Rajshahi, Bangladesh, Feb. 2018, pp. 1–6.
[37] J. Lorincz, I. Bule, and M. Kapov, "Performance analyses of renewable and fuel power supply systems for different base station sites," *Energies*, vol. 7, no. 12, pp. 7816–7846, Nov. 2014.
[38] M. H. Alsharif, "Techno-economic evaluation of a stand-alone power system based on solar power/batteries for global system for mobile communications base stations," *Energies*, vol. 10, no. 3, pp. 1–20, Mar. 2017.
[39] A. Jahid, K. H. Monju, S. Hossain, and F. Hossain, "Hybrid power supply solutions for off-grid green wireless networks," *Int. J. Green Energy*, vol. 16, no. 1, pp. 12–33, Jan. 2019.
[40] D. Bezmalinović, F. Barbir, and I. Tolj, "Techno-economic analysis of PEM fuel cells role in photovoltaic-based systems for the remote base stations," *Int. J. Hydrogen Energy*, vol. 38, no. 1, pp. 417–425, Jan. 2013.
[41] D. N. Luta and A. K. Raji, "Renewable hydrogen-based energy system for supplying power to telecoms base station," *Int. J. Eng. Res. Afr.*, vol. 43, pp. 112–126, Jun. 2019.
[42] V. A. Ani and A. N. Nzeako, "Potentials of optimized hybrid system in powering off-grid macro base transmitter station site," *Int. J. Renew. Energy Res.*, vol. 3, no. 4, pp. 861–871, Dec. 2013.
[43] M. Alsharif and J. Kim, "Hybrid off-grid SPV/WTG power system for remote cellular base stations towards green and sustainable cellular networks in South Korea," *Energies*, vol. 10, no. 1, p. 9, Dec. 2016.
[44] S. Singh, M. Singh, and S. C. Kaushik, "A review on optimization techniques for sizing of solar-wind hybrid energy systems," *Int. J. Green Energy*, vol. 13, no. 15, pp. 1564–1578, Dec. 2016.
[45] A. Jahid, M. K. H. Monju, M. E. Hossain, and M. F. Hossain, "Renewable energy assisted cost aware sustainable off-grid base stations with energy cooperation," *IEEE Access*, vol. 6, pp. 60900–60920, 2018.
[46] A. Bin Shams, A. Jahid, and M. F. Hossain, "A CoMP based LTE—A simulator for green communications," in *Proc. Int. Conf. Wireless Commun., Signal Process. Netw. (WiSPNET)*, Chennai, India, Mar. 2017, pp. 1751–1756.
[47] A. Jahid, A. B. Shams, and M. F. Hossain, "Green energy driven cellular networks with JT CoMP technique," *Phys. Commun.*, vol. 28, pp. 58–68, Jun. 2018.
[48] A. Jahid, A. B. Shams, and M. F. Hossain, "PV Powered CoMP based green cellular networks with standby grid supply," *Int. J. Photoenergy*, vol. 2017, pp. 1–14, Apr. 2017.
[49] C. Liu and B. Natarajan, "Power management in heterogeneous networks with energy harvesting base stations," *Phys. Commun.*, vol. 16, pp. 14–24, Sep. 2015.
[50] M. H. Alsharif, "Comparative analysis of solar-powered base stations for green mobile networks," *Energies*, vol. 10, no. 8, p. 1208, Aug. 2017.
[51] M. J. Farooq, H. Ghazzai, A. Kadri, H. El Sawy, and M.-S. Alouini, "A hybrid energy sharing framework for green cellular networks," *IEEE Trans. Commun.*, vol. 65, no. 2, pp. 918–934, Feb. 2017.
[52] Y. K. Chia, S. Sun, and R. Zhang, "Energy cooperation in cellular networks with renewable powered base stations," *IEEE Trans. Wireless Commun.*, vol. 13, no. 12, pp. 6996–7010, Dec. 2014.
[53] A. Jahid, A. B. Shams, and M. F. Hossain, "Energy cooperation among BS with hybrid power supply for DPS CoMP based cellular networks," in *Proc. 2nd Int. Conf. Electr., Comput. Telecommun. Eng. (ICECTE)*, Rajshahi, Bangladesh, Dec. 2016, pp. 1–4.
[54] J. Leithon, T. J. Lim, and S. Sun, "Energy exchange among base stations in a cellular network through the smart grid," in *Proc. IEEE Int. Conf. Commun. (ICC)*, Sydney, NSW, Australia, Jun. 2014, pp. 4036–4041.
[55] A. Antonopoulos, E. Kartsakli, A. Bousia, L. Alonso, and C. Verikoukis, "Energy-efficient infrastructure sharing in multi-operator mobile networks," *IEEE Commun. Mag.*, vol. 53, no. 5, pp. 242–249, May 2015.
[56] A. Bousia, E. Kartsakli, A. Antonopoulos, L. Alonso, and C. Verikoukis, "Game-theoretic infrastructure sharing in multioperator cellular networks," *IEEE Trans. Veh. Technol.*, vol. 65, no. 5, pp. 3326–3341, May 2016.
[57] A. Jahid, M. S. Hossain, M. K. H. Monju, M. F. Rahman, and M. F. Hossain, "Techno-economic and energy efficiency analysis of optimal power supply solutions for green cellular base stations," *IEEE Access*, vol. 8, pp. 43776–43795, 2020.
[58] M. S. Hossain, M. Rahman, M. T. Sarker, M. E. Haque, and A. Jahid, "A smart IoT based system for monitoring and controlling the sub-station equipment," *Internet Things*, vol. 7, Sep. 2019, Art. no. 100085.
[59] M. H. Alsharif, R. Nordin, and M. Ismail, "Green wireless network optimisation strategies within smart grid environments for long term evolution (LTE) cellular networks in Malaysia," *Renew. Energy*, vol. 85, pp. 157–170, Jan. 2016.
[60] G. Auer, V. Giannini, C. Desset, I. Godor, P. Skillermark, M. Olsson, M. Imran, D. Sabella, M. Gonzalez, O. Blume, and A. Fehske, "How much energy is needed to run a wireless network?" *IEEE Wireless Commun.*, vol. 18, no. 5, pp. 40–49, Oct. 2011.
[61] H. Holtkamp, G. Auer, V. Giannini, and H. Haas, "A parameterized base station power model," *IEEE Commun. Lett.*, vol. 17, no. 11, pp. 2033–2035, Nov. 2013.

MD. SANWAR HOSSAIN (Student Member, IEEE) received the B.Sc. degree in electrical and electronic engineering (EEE) from the Rajshahi University of Engineering and Technology, Rajshahi, Bangladesh, in 2010. He is currently pursuing the M.Sc. degree in electrical, electronic, and communication engineering with the Military Institute of Science and Technology (MIST). From 2011 to 2015, he was a Lecturer, and he is currently serving as an Assistant Professor with the Department of EEE, Bangladesh University of Business and Technology, Dhaka, Bangladesh. His research interests include green energy, smart grids, and power system optimization.

ABU JAHID (Student Member, IEEE) received the bachelor's and M.Sc. degrees in electrical engineering from the Military Institute of Science and Technology (MIST), Dhaka, Bangladesh. He is currently pursuing the Ph.D. degree with the Department of Electrical and Computer Engineering, University of Ottawa, Canada. From 2010 to 2012, he worked as a BSS Engineer with Huawei Technologies, where he studied on radio network planning and optimization. He was an Assistant Professor with the Department of Electrical and Electronic Engineering (EEE), Bangladesh University of Business and Technology, Dhaka, from 2016 to 2019. His research interests include green cellular networking, photonic integrated circuits, and microwave photonics. He has been serving as TPC member and a reviewer of many reputed international journals and conferences.

KHONDOKER ZIAUL ISLAM received the B.Sc. and M.Sc. degrees in electrical engineering from the Islamic University of Technology (IUT), Bangladesh. He is currently pursuing the Ph.D. degree with the Bangladesh University of Engineering and Technology (BUET), Dhaka, Bangladesh. He is an Assistant Professor with the Department of Electrical and Electronic Engineering, Bangladesh University of Business and Technology (BUBT), Dhaka. His current research interests include C-RAN, 5G cellular networks, green communication, radio resource management, and radio planning for cellular networks.

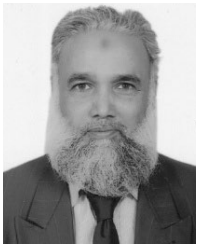

MD. FAYZUR RAHMAN was born in Thakurgaon, Bangladesh, in 1960. He received the B.Sc.Eng. degree in electrical and electronic engineering from Rajshahi Engineering College, Bangladesh, in 1984, the M.Tech. degree in industrial electronics from the S. J. College of Engineering, Mysore, India, in 1992, and the Ph.D. degree in energy and environment electromagnetics from Yeungnam University, South Korea, in 2000. He was a Professor in electrical and electronic engineering at the Rajshahi University of Engineering and Technology (RUET) and served as the HOD of the same department. He also served as the Departmental Head for two years at the Department of Electrical and Electronic Engineering (EEE) and two years at the Department of ETE with Daffodil International University. He is currently a Professor and the Chairperson in the Department of EEE, Green University of Bangladesh. His current research interests are energy and environment electromagnetics, electronics and machine control, and high voltage discharge applications. He is a Fellow of the Institution of Engineer's (IEB), Bangladesh, and a Life Member of the Bangladesh Electronic Society.